Mutation Research - Genetic Toxicology and Environmental Mutagenesis 900 (2024) 503835

Contents lists available at ScienceDirect

Mutation Research - Genetic Toxicology and Environmental Mutagenesis

journal homepage: www.elsevier.com/locate/gentox

In vitro hepatic 3D cell models and their application in genetic toxicology: A systematic review

Martina Štampar, Bojana Žegura *

National Institute of Biology, Department of Genetic Toxicology and Cancer Biology, Večna pot 121, Ljubljana 1000, Slovenia

A R T I C L E I N F O

Keywords:
Genotoxicity
Advanced 3D in vitro models
Hepatic cells
Spheroids
Comet assay
Micronucleus assay

A B S T R A C T

The rapid development of new chemicals and consumer products has raised concerns about their potential genotoxic effects on human health, including DNA damage leading to serious diseases. For such new chemicals and pharmaceutical products, international regulations require genotoxicity data, initially obtained through *in vitro* tests, followed by *in vivo* experiments, if needed. Traditionally, laboratory animals have been used for this purpose, however, they are costly, ethically problematic, and often unreliable due to species differences. Therefore, innovative more accurate *in vitro* testing approaches are rapidly being developed to replace, refine and reduce (3R) the use of animals for experimental purposes and to improve the relevance for humans in toxicology studies. One of such innovative approaches are *in vitro* three-dimensional (3D) cell models, which are already being highlighted as superior alternatives to the two-dimensional (2D) cell cultures that are traditionally used as *in vitro* models for the safety testing of chemicals and pharmaceuticals. 3D cell models provide physiologically relevant information and more predictive data for *in vivo* conditions. In the review article, we provide a comprehensive overview of 3D hepatic cell models, including HepG2, HepG2/C3A, HepaRG, human primary hepatocytes, and iPSC-derived hepatocytes, and their application in the field of genotoxicology. Through a detailed literature analysis, we identified 31 studies conducted between 2007 and April 2024 that used a variety of standard methods, such as the comet assay, the micronucleus assay, and the γH2AX assay, as well as new methodological approaches, including toxicogenomics, to assess the cytotoxic and genotoxic activity of chemicals, nanoparticles and natural toxins. Based on our search, we can conclude that the use of *in vitro* 3D cell models for genotoxicity testing has been increasing over the years and that 3D cell models have an even greater potential for future implementation and further refinement in genetic toxicology and risk assessment.

1. Introduction

The increasing development of new chemicals and consumer products (e.g., pharmaceuticals, cosmetics, food and feed additives and other everyday products) has raised concern about their potential adverse effects on human health, in particular, in terms of genotoxicity [1–4]. Genotoxic chemicals pose a considerable threat to human health by inducing DNA damage. This can result in cytotoxic effects such as cell death or accelerated ageing, or genotoxic effects that may contribute to the onset of diseases such as cancer, chronic diseases, reproductive disorders, infertility, heritable diseases, malformations in offspring, neurodegenerative disorders, and other health-related problems [5,6]. For the registration and authorisation of chemicals and pharmaceutical products, international regulations and guidelines require genotoxicity data, which are obtained in the first step through a series of *in vitro* tests with bacteria, and mammalian cells, and if the results are positive, further *in vivo* experiments are required to assess the risk to human health [4,7–9]. In the past, laboratory animals have widely been used for routine testing [10–12]. The cost of using standard animal testing to assess the safety of chemicals worldwide is approximately 13 billion euros annually, and more than 100 million experimental animals are sacrificed for chemical safety testing [13,14], which is ethically critical. In addition, due to differences between species, it is difficult to predict findings from animal models to humans [11,15,16]. A meta-analysis of data on genotoxicity testing of chemicals showed that 90 % of the positive results obtained with currently used *in vitro* test systems on bacteria and mammalian cell lines are false positives [14,17]. This again indicates that a large number of experimental animals are being unnecessarily sacrificed, raising ethical concerns and highlighting the importance of minimising the use of animals in such testing practices,

* Corresponding author.
E-mail address: bojana.zegura@nib.si (B. Žegura).

https://doi.org/10.1016/j.mrgentox.2024.503835
Received 13 July 2024; Received in revised form 24 October 2024; Accepted 7 November 2024
Available online 12 November 2024

which could be avoided by more reliable *in vitro* testing systems [18–20]. This is why, in the 21st century, several research agencies worldwide have started to discuss a paradigm shift in toxicology towards the development of alternative approaches to animal experimentation that would provide the same or even more human-relevant information than animal experiments [21,22].

Currently, the use of laboratory animals for research purposes and the protection of their well-being and welfare is regulated by the European Union legislation Directive on the protection of animals used for scientific purposes (2010/63). The European Union's REACH program (Registration, Evaluation, Authorisation and Restriction of Chemical Substances, 2007/2006) actively promotes the use of non-animal methods for chemical testing. Similarly, the US Environmental Protection Agency (EPA) plans to eliminate the use of animal models in testing chemicals and pesticides by 2035 (US EPA, 2020). Although there is considerable investment in the 3R principles – Reduce, Replace and Refine – there is a certain reluctance to fully embrace alternative approaches, due to remaining challenges in standardization, quality control and validation [8,23–25]. All these facts highlight the urgent need to develop physiologically relevant human-derived hepatic models to replace the use of animals for experimental purposes to test chemicals, taking into account the continuous development of chemicals and drugs [10,16,20,22,26,27].

In the field of preclinical testing, the OECD guidelines indicate that genotoxicity assessment is predominantly performed using 2D monolayer cultures. These include metabolically deficient rodent cell lines such as Chinese hamster lung cells (V79) and mouse lymphoma cells (L5178Y), as well as various human cell lines including primary human hepatocytes (PHH), hepatic cancer cell lines, immortalized hepatic cells, and stem cell-derived hepatocyte-like cells (HLC) [14]. Since most genotoxic carcinogens in humans require metabolic activation, *in vitro* cell models should mimic human metabolism, in particular liver metabolism, as closely as possible. However, metabolic activation, especially in metabolically deficient models (bacteria and non-hepatic cell lines), is typically studied by adding an induced S9 fraction of rat or hamster liver, comprising the major isoforms of cytochrome P450 and other metabolic enzymes, to the compounds under study during incubation [28,29]. The use of the rat liver fraction is, however, questionable for the prediction of mutagenicity in humans, as the metabolic characteristics are species-specific. Therefore, metabolically competent human cell models particularly those of hepatic origin should be used for chemical hazard assessment. However, standard hepatic 2D cell-based cultures often fall short, failing to predict human responses effectively. This highlights the urging need for more sophisticated and physiologically relevant cell models in early drug testing phases to improve safety and efficacy outcomes [30–32].

Hepatic cell lines cultured in monolayer (2D) systems often exhibit metabolic deficiencies, characterized by a lack of crucial metabolic enzymes, numerous limitations, and poor correlation with *in vivo* conditions. One of the main limitations is the lack of numerous biological functions such as cell-cell and cell-matrix interactions, resulting in decreased cell differentiation, flattened cell morphology with the altered cytoskeleton, reduced cell viability, altered cell signalling pathways, and most importantly, as already mentioned, the reduction or loss of expression many hepatic enzymes (phase I and II) involved in the metabolism of xenobiotic substances. However, the metabolic capacity of a cell model is a crucial requirement for a valid model in genetic toxicology, and it is also important that the *in vitro* model resembles the *in vivo* phenotype. All of these shortcomings of culturing cells in two dimensions result in significantly different cell behaviour from *in vivo* conditions, leading to inaccurate pharmacological or toxicological results [31,33,34]. Human primary hepatocytes (hPH) are still considered the gold standard for liver toxicity and metabolism of xenobiotics [35,36]. However, hPH are not suitable for routine genotoxicity testing in particular long-term studies due to their limited availability, short life span, genetic and metabolic variability between donors, rapid dedifferentiation and loss of hepatocyte functions and hepatic phenotype in two-dimensional (2D) culture, lack of proliferative capacity in 2D cultures, and high cost [37,38]. As an alternative, several human hepatocellular carcinoma cell lines (e.g., HepG2, HepG2/C3A, Huh-6, Huh-7, HepaRG) have been established [27,39,40], characterised and widely used to assess genotoxicity of various compounds [27,41–43]. These cell lines combine the advantages of an unlimited lifespan, high availability, easy handling and high reproducibility of experimental results due to a stable phenotype, and are of human origin [36], yet they also have a number of drawbacks, the most notable of which is a deficient metabolism [27].

We have conducted a comprehensive review of the literature published from 2007 to April 2024 on the application of *in vitro* 3D hepatic models (spheroids) in the assessment of DNA damage. First, we provided an overview of the main hepatic cell types commonly used for spheroid formation, discussing their formation describing their advantages over 2D cultures and the specific limitations of certain cell types (Table 1). We also described techniques used to form spheroids for genotoxicity assessment, highlighting their respective advantages and disadvantages (Table 2). Additionally, we collected extensive data on cytotoxicity (Table 3) and genotoxicity (Table 4) endpoints. The tables summarize the most frequently used human hepatic cell types for testing the (cyto) genotoxic effects of various chemicals, nanoparticles, and natural toxins. Furthermore, we gathered data on the chemicals tested, exposure durations, and studied endpoints along with a discussion of future research directions. Relevant articles were searched in the Web of Science database, which includes articles from the following citation indexes; Science Citation Index Expanded (SCI-EXPANDED), Social Sciences Citation Index (SSCI), Arts & Humanities Citation Index (A&HCI), Conference Proceedings Citation Index-Science (CPCI-S) and Conference Proceedings Citation Index-Social Science & Humanities (CPCI-SSH), and the Google scholar database. The following keywords and corresponding logical operators (AND, OR and NOT) were used in the search: "3D models", "spheroids", "Hepatic cells", "HepG2", "Huh6", "Huh7", "HepaRG", "HPP", "DNA damage" and "Viability". This resulted in 31 relevant hits of the scientific papers. The sample was obtained in April 2024.

Table 2 summarizes the most commonly used methods for spheroid formation that have been used in studies to assess DNA damage. These techniques include the Ultra-Low Attachment (ULA) Plate method, the Hanging Drop method, the Forced Floating method, the Aggrewell (micro-modelling) method, and the dynamic bioreactor approach. In the studies analysed, the maturation period before treatment varies according to the spheroid formation technique chosen. Under static conditions, spheroids typically mature for 3–5 days and in some studies maturation period of 7–8 days has been used, whereas under dynamic conditions the maturation period can be extended to several weeks or even months.

2. *In vitro* three-dimensional (3D) cell models

In the last decade, there has been a notable increase in the development and use of three-dimensional (3D) cell models in toxicology, which are nowadays already considered as improved pre-clinical testing systems and are recognized as promising *in vitro* alternatives to animal testing [26,44,45]. Their development and advancement have significantly expanded their application in a variety of fields, encompassing research on cancer cell processes, intracellular interactions, cell differentiation, organ development, disease modelling, and drug development and screening [46–49]. In addition, there is a growing trend towards the application of 3D cell models in genetic toxicology and risk assessment [26,31]. Nowadays, it is well known and proven that hepatic 3D cell models, compared to traditional hepatic 2D monolayer cell cultures, have improved cell-cell and cell-extracellular matrix interactions, as well as tissue-like structures, and very importantly, have improved metabolic activity and hepatic function, thus providing more relevant *in*

Table 1
Advantages of 3D cell models developed from the most frequently used hepatic cell types over traditional 2D models used for genotoxicity assessment and limitations of these hepatic cell types.

Cell type	Advantages of 3D models over traditional 2D models	Limitation of hepatic cell types	References
HepG2	- Easy to culture - Low cost - Increased expression of several metabolic enzymes (phase I, II), - Expression of liver-specific functions - Functional nuclear receptors, e.g., CAR and RXR - p53-proficient - Increased albumin synthesis compared to 2D - Increased secretion of urea compared to 2D models	- Simplified architecture (only one type of cell) - Low glutathione synthesis - Carcinogenic origin - Abnormal karyotype (modal number = 55 (range = 50–60)) - Inconsistent albumin production - Incomplete hepatic differentiation	[31, 66–68]
HepG2-C3A (subclone derived from HepG2 – herein designated C3A cells)	- Easy to culture - Low cost - Strong contact-inhibited growth characteristics - Enhanced albumin secretion and cytochrome P450 enzyme activity compared to the parent 2D HepG2 line - Increased expression of several metabolic enzymes (phase I, II), nuclear receptors - p53-proficient - Ability to grow in glucose-deficient media -Lower carcinogenic/ tumorigenic potential compared to 2D HepG2	- Simplified architecture (only one type of cells) - Carcinogenic origin - Abnormal karyotype - Less efficient capacity to detoxify ammonia - Inconsistent albumin production - Incomplete hepatic differentiation	[31,42, 69–72]
HepaRG	- Increased urea and albumin secretion compared to 2D - Enhanced albumin secretion and cytochrome P450 enzyme activity compared to the parent 2D HepaRG line - Increased expression of several metabolic enzymes (phase I, II), nuclear receptors - p53-proficient - Exhibits liver-specific functions - More sensitive to hepatotoxic compounds, allowing for accurate toxicity testing	- High cost - Culture Complexity - Incomplete hepatic differentiation - Slow maturation - Low division on cells in culture	[26, 73–79]
Human primary hepatocytes	- Maintain longer functional phenotype and metabolic enzyme expression - Potential for higher sensitivity to certain toxins compared to other non-primary cell types - Longevity and Stability (up to 7 weeks) - Non-carcinogenic origin	- Low human tissue availability - High cost - Variable enzyme activity over time - Low GSTP1 expression - Rapid dedifferentiation and loss of function - Donor/patient specific	[73,74, 80–83]
iPSC-derived hepatocytes	- More mature phenotype - Increased expression of metabolic enzymes (phase I, II) - p53-proficient - Increased urea and albumin secretion - Potential for higher sensitivity to certain toxins - Non-carcinogenic origin (normal karyotype)	- Very expensive - Long differentiation and maturation period - Seeding density-dependent phenotype - Labor intensive: for each experiment, differentiation and maturation must be done from the beginning	[73, 84–88]

vivo-like responses in terms of cell viability, proliferation, differentiation, morphology, gene and protein expression and cell function [26,39, 50–53].

Several 3D cell models have been developed, ranging from basic spheroid cultures with one type of cells [39,54–56] to more complex systems such as organoids [48,57] and micro physiological systems [31, 37,47,58]. A distinctive advantage of 3D cell models is that they can provide physiologically relevant information and more predictive data for *in vivo* conditions compared to 2D culture systems.

This review summarizes the outcomes of studies that have used 3D hepatic cell models to study DNA damage caused by a wide range of chemicals, nanoparticles and natural toxins, using a variety of standard genotoxicity assays, including the micronucleus, comet and γH2AX assays, as well as some novel methodological approaches, including transcriptomics (screening for modifications and alterations in gene expression profiles) to assess mechanisms of action, to provide scientific data to evaluate the suitability of 3D hepatic cell models for genotoxicity testing (Table 4). The analysis of the dataset indicates that the earliest published papers are from 2008 and 2016. Over the past few years, there has been a gradual increase in the number of publications documenting the application of 3D hepatocellular models for DNA damage assessment, from 2 published papers in 2008 and 2016–31 published articles until April 2024. These findings indicate that the field of study is relatively new, and the increase in research activity highlights the importance and interest in the development and application of 3D hepatic cell models for genotoxicity assessment.

3. Most frequently used hepatic cell types and methods for spheroid formation to assess cytotoxic and genotoxic activities of chemicals and nanoparticles

The development of hepatic 3D *in vitro* cell models and their application in the field of genetic toxicology is a dynamic and rapidly evolving field that is still in its infancy. This field holds great promise for

Table 2
The most frequently applied technique for the formation of spheroids used for genotoxicity assessment.

Spheroid forming methods	Advantages	Disadvantages	References
Ultra-low attachment plates method (ULA) (96- U or V- bottom well-liquid overlay) Initial cell density*: 650–20.000 cells/well depending on cell type (Fig. 1A)	- Large-scale spheroid production - Easy handling (no need to be trained in handling) - No specialized materials and equipment - Inexpensive.	- Difficulty in forming tight, uniform spheroids - No direct contact between cells and extracellular matrix - Long-term culture difficult (more than 14 days) - The risk of rapid occurrence of necrotic core - Long-term culture difficult.	[61,89–93]
Hanging drop method Initial cell density*: 4000–30.000 cells/20 μL drop depending on cell type (Fig. 1B)	- Large-scale spheroid production - Uniform spheroids (same size, same shape) - No specialized materials and equipment - Inexpensive.	- Difficult to track spheroid formation - Time-consuming to change media and treatment - Risk of droplet dehydration - Difficulty in scale-up - Long-term culture difficult (more than 14 days) - The risk of rapid occurrence of necrotic core - Long-term culture difficult.	[91,92, 94–96]
Forced floating method (96- U or V- bottom well, centrifugation) Initial cell density*: 650–20.000 cells/well depending on cell type (Fig. 1C)	- Large-scale spheroid production - Easy handling - Uniform spheroids (same size, same shape) - No specialized materials and equipment - Inexpensive.	- Time-consuming to change media and treatment - Difficulty in scale-up - Long-term culture difficult (more than 14 days) - The risk of rapid occurrence of necrotic core - Long-term culture difficult.	[66,97,98]
Aggrewell method (Micromodeling, centrifugation) for the formation of spheroids/aggregates Initial cell density*: $1,2x10^4$–$1,2x10^6$ depending on cell type (Fig. 1D)	- Large-scale spheroid production - Easy handling - Uniform spheroids (same size, same shape) - Better efficiency	- The risk of rapid occurrence of necrotic core - Long-term culture difficult	[39,42]
Dynamic Bioreactor method Spheroids in one BR: 100–600 depending on cell type (Fig. 1E)**	- Large-scale spheroid production - Uniform (size and shape) spheroids - Long-term culture (allows prolonged chronic exposures for more than several weeks) - Better diffusion of nutrients, growth factors, and oxygen supply into the spheroid (reduced formation of necrotic core) - Better excretion of waste products, CO_2 from the spheroid	- Expensive material - Specialized equipment - Time-consuming and labor-intensive method	[39,42,99]

The table summarizes the initial cell densities* and the number of spheroids per one bioreactor** reported in selected articles that utilize 3D culture techniques for cytogenotoxicity assessments.

advancing our understanding of genotoxic effects and offers new perspectives in an area where traditional approaches have reached their limits. Initially, hepatocellular 3D cell models were mainly used for drug development and pharmacological research. However, significant progress has recently been made in the development of 3D cell models and in particular their use to investigate genotoxic effects such as primary DNA damage [42,51,56,59,60] and chromosomal instability [61] induced by chemicals [42,43,59,61,62], nanoparticles [51,63], and natural toxins [41].

The analysis of the literature data on this research topic showed that hepatic 3D *in vitro* systems are mainly presented in the form of spheroids. The most frequently utilized cell types for assessing DNA damage are the HepG2 and HepG2/C3A cells, followed by HepaRG cells. Table 1 summarizes the advantages of 3D hepatic cell models, developed from the most commonly used hepatic cell types, over traditional 2D models in genetic toxicology research, along with the limitations of these hepatic cell types. Additionally, a few studies assessing long-term toxicity in 3D systems using primary human hepatocytes have been reported, and one study involving iPSC-derived hepatocytes was encountered, however, to our knowledge there are no published data on the use of these two cell types in 3D conformation for genotoxicity assessment. Other hepatic cell lines such as HUH6/7, Hep3B, JHH6, which are in the traditional two-dimensional format commonly used to study DNA damage, have not yet been used in 3D *in vitro* systems.

Forming spheroids with optimal characteristics such as normal karyotype, high cell metabolic activity, properly functioning repair mechanisms and others that can be routinely used for genotoxicity testing is challenging. Hence, various methods and technologies have been developed where cells are grown under static and dynamic conditions in more complex environments, such as agitation-based approaches, hanging drop cultures, microfluidic cell culture platforms, bioreactors, microchips (organs-on-chip), hydrogels, matrices, and scaffolds [64,65]. These techniques have been successfully employed in drug development, however, most of them have not yet been systematically verified and validated for their suitability for use in genetic toxicology to study whether chemicals, nanoparticles and complex mixtures cause DNA damage and to study their mechanisms of action.

4. Methodological approaches for genotoxicity assessment on hepatic spheroids

Our systematic review revealed that the most widely applied methods for determining genotoxicity of chemicals and nanoparticles on hepatic spheroids were the comet assay (alkaline [26,66,100] and high-throughput CometChip [73,101]) and the micronucleus assay [61,67,102] followed by the γ-H2AX method [103] (Table 4). These methods are sensitive and valuable tools for the assessment of primary DNA damage and chromosomal instability and for studying the mechanisms of action of various chemicals and nanoparticles. Prior to

Table 3
Studies describing the use of 3D cell models to analyse viability, proliferation and oxidative stress caused by chemicals, nanoparticles or natural toxins. The table includes information on the cell model, method of spheroid formation, maturation time, endpoints determined, compounds tested, duration of exposure and effects observed.

Cell line	Method for spheroid formation	Time before treat-ment	End-point	Assay	Chemical/ nanoparticle (NP)/ microplastic (MP) tested	Concentration range	Exposure time/ Effect/LOAEC							R
							30m/ 3h/6h	24 h	48 h	72 h	96 h	120 h	6d/7d/9d/ 14d/21d+	
HepG2	Ultra-low attachment plates (ULA) (96-U-well)	1 day	Viability	MTT assay	Cisplatin	2.5–10 mg/L			5 mg/L					[104]
					5-fluorouracil	12.5–100 mg/L			100 mg/L					
					Adriamycin	0.30–2.5 mg/L			1.25 mg/ L					
HepG2	Hanging drop	3 days	Viability	Trypan Blue	NP: TiO_2	0.2–10 µg/ml		neg.				neg.		[63]
					NP: ZnO	0.2–10 µg/ml		neg.				10 µg/ ml		
					NP: Ag	0.2–10 µg/ml		neg.				neg.		
					NP: $BaSO_4$	0.2–10 µg/ml		5 µg/ml				neg.		
					NP: CeO_2	0.2–10 µg/ml		neg.				neg.		
HepG2	Hanging drop	4 days	Viability	Alamar blue assay	NP: TiO_2	1–75 µg/cm^2		neg.						[51]
					NP: Ag	1–30 µg/cm^2		3 µg/ cm^2						
					NP: ZnO	1–30µg/cm^2		30 µg/ cm^2						
HepG2	Hanging drop	4 days + one week in 96 well plate	Viability	Alamar Blue	COL	1–750 µM		neg.						[56]
					CHLO	1–750 µM		100 µM						
					MMS	1–750 µM		neg.						
HepG2	Forced floating (96-U-well)	3 days	Viability	MTS assay	BPA	24 h: 10–80 µM; 96 h:1–8 µM		neg.			neg.			[105]
					BPC	24 h: 10–80 µM; 96 h:1–8 µM		40 µM			neg.			
					BPAP	24 h: 10–80 µM; 96 h:1–8 µM		20 µM			neg.			
					BPA + BPC	24 h: 10 + 10, 20 + 20, 40 + 40 µM; 96 h: 1 + 1, 2 + 2, 4 + 4 µM		40 + 40 µM			neg.			
					BPA + BPAP	24 h: 10 + 10, 20 + 20, 40 + 40 µM; 96 h: 1 + 1, 2 + 2, 4 + 4 µM		neg.			4 + 4 µM			
HepG2	Forced floating (96-U-well)	3 days	Viability	MTS assay	B(a)P	24 h: 0.1–40 µM; 72 h: 0.001–10 µM		neg.		neg.				[62]
					PhIP	24 h: 50–200 µM; 72 h: 25–200 µM		neg.		400 µM				
HepG2	Forced floating (96-U-well)	3 days	Viability	MTS assay	B(a)P	10–40 µM		40 µM						[66]
					AFB1	10–40 µM		40 µM						
					PhIP	50–200 µM		200 µM						
					IQ	50–250 µM		50 µM						
					ET	0.17–17 µM		neg.						
HepG2	Forced floating (96-U-well)	3 days	Viability	MTS assay/ Planimetry	BPA	24 h: 5–160 µM; 96 h: 2.5–80 µM		neg.			neg.			[60]
					BPS	24 h: 5–160 µM; 96 h: 2.5–80 µM		neg.			neg.			
					BPAP	24 h: 10–80 µM; 96 h:1–8 µM		neg.			neg.			
					BPAF	24 h: 5–160 µM; 96 h: 2.5–80 µM		neg.			neg.			

(*continued on next page*)

Table 3 (*continued*)

Cell line	Method for spheroid formation	Time before treat-ment	End-point	Assay	Chemical/ nanoparticle (NP)/ microplastic (MP) tested	Concentration range	Exposure time/ Effect/LOAEC							R
							30m/ 3h/6h	24 h	48 h	72 h	96 h	120 h	6d/7d/9d/ 14d/21d+	
					BPFL	24 h: 5–160 µM; 96 h: 2.5–80 µM		160 µM			80 µM			
					BPC	24 h: 5–160 µM; 96 h: 2.5–80 µM		neg.			80 µM			
HepG2	Forced floating (96-U-well)	3 days	Viability	MTS assay	CYN	0.125–0.5 µg/ml				neg.				[41]
HepG2	Alginate scaffolds in 6 well plates	5 days	Viability	PrestoBlue	AVA	0–500 µM		18 µM	18 µM	10 µM				[106]
HepG2	Method not specified	3 days + 11 days	Viability	MTT assay	NP: FeO	1–100 µg/ml		10 µg/ ml						[107]
					NP: CFO	1–100 µg/ml		25 µg/ ml						
					NP: NFO	1–100 µg/ml		10 µg/ ml						
					NP: ZFO	1–100 µg/ml		25 µg/ ml						
HepG2	Hanging drop	3 days	proliferation	Cytokinesis-block proliferation index (CBPI)	AFB1	0.01–0.2 µM		neg.				/		[67]
					MMS	5–30 µM		neg.				/		
					NP: ZnO	0.2–2 µg/ml		/				neg.		
					AFB1	0.1 µM		/				0.1 µM		
HepG2	Hanging drop	4 days	proliferation	Cytokinesis-block proliferation index (CBPI)	B(a)P	2–8 µM		neg.						[61]
					PhIP	5–15 µM		neg.						
HepG2	Forced floating (96-U-well)	3 days	proliferation	Ki67	B(a)P	24 h: 0.1–40 µM; 72 h: 0.001–10 µM		20 µM		1 and 10 µM				[62]
					PhIP	24 h: 50–200 µM; 72 h: 25–200 µM		200 µM		neg.				
HepG2	Forced floating (96-U-well)	3 days	proliferation	Ki67	BPA	24 h: 0.1–40 µM; 96 h: 0.01–10 µM		neg.			neg.			[60]
					BPS	24 h: 0.1–40 µM; 96 h: 0.01–10 µM		neg.			neg.			
					BPAP	24 h: 0.1–40 µM; 96 h: 0.01–10 µM		neg.			neg.			
					BPAF	24 h: 0.1–40 µM; 96 h: 0.01–10 µM		neg.			neg.			
					BPFL	24 h: 0.1–40 µM; 96 h: 0.01–10 µM		10 µM			10 µM			
					BPC	24 h: 0.1–40 µM; 96 h: 0.01–10 µM		40 µM			10 µM			
HepG2	Forced floating (96-U-well)	3 days	proliferation	Ki67	CYN	0.125–0.5 µg/ml				neg.				[41]
HepG2	Forced floating (96-U-well)	3 days	Cell cycle arrest	Flow cytometry (Hoechst 33258 dye)	B(a)P	24 h: 0.1–40 µM; 72 h: 0.001–10 µM		20 µM		10 µM				[62]
					PhIP	24 h: 50–200 µM; 72 h: 25–200 µM		200 µM		200 µM				
HepG2	Forced floating (96-U-well)	3 days	Cell cycle arrest	Flow cytometry (Hoechst 33258 dye)	BPA	24 h: 0.1–40 µM; 96 h: 0.01–10 µM		neg.			0.01 µM			[60]
					BPS	24 h: 0.1–40 µM; 96 h: 0.01–10 µM		neg.			neg.			
					BPAP	24 h: 0.1–40 µM; 96 h: 0.01–10 µM		neg.			10 µM			
					BPAF	24 h: 0.1–40 µM; 96 h: 0.01–10 µM		neg.			10 µM			

(*continued on next page*)

Table 3 (*continued*)

Cell line	Method for spheroid formation	Time before treat-ment	End-point	Assay	Chemical/ nanoparticle (NP)/ microplastic (MP) tested	Concentration range	Exposure time/ Effect/LOAEC							R
							30m/ 3h/6h	24 h	48 h	72 h	96 h	120 h	6d/7d/9d/ 14d/21d+	
					BPFL	24 h: 0.1–40 µM; 96 h: 0.01–10 µM		40 µM			neg.			
					BPC	24 h: 0.1–40 µM; 96 h: 0.01–10 µM		40 µM			neg.			
HepG2	Forced floating (96-U-well)	3 days	Cell cycle arrest	Flow cytometry (Hoechst 33258 dye)	CYN	0.125–0.5 µg/ml				0.25 µg /ml				[41]
HepG2	Forced floating (96-U-well)	3 days	Oxidative stress	MDA	BPA	24 h: 10–40 µM; 96 h:1–4 µM		20 µM			2 µM			[105]
					BPC	24 h: 10–40 µM; 96 h:1–4 µM		40 µM			4 µM			
					BPAP	24 h: 10–40 µM; 96 h:1–4 µM		neg.			4 µM			
					BPA + BPC	24 h: 10 + 10, 20 + 20 µM; 96 h: 1 + 1, 2 + 2 µM		neg.			neg.			
					BPA + BPAP	24 h: 10 + 10, 20 + 20 µM; 96 h: 1 + 1, 2 + 2 µM		neg.			neg.			
HepG2	Forced floating (96-U-well)	3 days	Oxidative stress	DHE fluorescent probe	BPA	24 h: 10–40 µM; 96 h:1–4 µM		20 µM			2 µM			[105]
					BPC	24 h: 10–40 µM; 96 h:1–4 µM		40 µM			4 µM			
					BPAP	24 h: 10–40 µM; 96 h:1–4 µM		20 µM			2 µM			
					BPA + BPC	24 h: 10 + 10, 20 + 20 µM; 96 h: 1 + 1, 2 + 2 µM		20 + 20 µM			2 + 2 µM			
					BPA + BPAP	24 h: 10 + 10, 20 + 20 µM; 96 h: 1 + 1, 2 + 2 µM		20 + 20 µM			2 + 2 µM			
HepG2	Forced floating (96-U-well)	3 days	Oxidative stress	Q-PCR (mRNA expression of HIF−1a)	CYN	0.125–0.5 µg/ml				0.5 µg/ml upregulated for 2.13 fold				[41]
HepG2/C3A	Ultra-low attachment plates (ULA) (96-U-well)	7 days	Viability	Morphology	Diosgenin	10–40 µM				20 µM				[108]
HepG2/C3A	Cell-repellent microplates with agarose liquid overlay (LOT)	7 days	Viability	ATP assay	B(a)P 2-AA 4-NQO PhIP	0.1–100 µM 0.1–100 µM 0.1–100 µM 0.1–100 µM		neg. neg. 50 µM neg.						[109]
HepG2/C3A	Forced floating (96-U-well)	3 days	Viability	MTT assay	PLN	1, 2.5, 5, 10, 20, 40, 50 µM		20 µM						[98]
HepG2/C3A	Aggrewell + Clinostar	24 h + 21 days	Viability	ATP assay	B(a)P	24 h: 40 µM; 96 h: 4 µM		40 µM			4 µM			[42]
					PhIP	24 h: 200, 400 µM; 96 h: 100 µM		400 µM			neg.			
HepG2/C3A	Aggrewell + Clinostar	24 h + 17 days	Viability	ATP assay	Uzara	200, 250 mg/kg							**21d** neg.	[110]
HepG2/C3A	Forced floating (96-U-well)	3 days	Cell cycle arrest	PI staining flow cytometry	PLN	10–40 µM		10 µM						[98]
HepG2/C3A	Forced floating (96-U-well)	3 days	Oxidative stress	DCFDA (flow cytometry)	PLN	10–40 µM		20 µM						[98]

(*continued on next page*)

Table 3 (*continued*)

Cell line	Method for spheroid formation	Time before treat-ment	End-point	Assay	Chemical/ nanoparticle (NP)/ microplastic (MP) tested	Concentration range	Exposure time/ Effect/LOAEC							R
							30m/ 3h/6h	24 h	48 h	72 h	96 h	120 h	6d/7d/9d/ 14d/21d+	
HepaRG	Ultra-low attachment plates (ULA) (96-U-well)	5 days	Viability	MTT assay	NP: Ag	5, 50 µg/ml	**6 h** 50 µg/ml	5 µg/ml						[111]
HepaRG	Ultra-low attachment plates (ULA) (96-U-well)	8 days	Viability	ATP assay	NP: TiO_2	0.31–31.25 µg/cm^2	/	neg.	neg.					[93]
					NP: ZnO S	0.031–31.25 µg/cm^2	50 µg/ ml	/	/					
					NP: ZnO NM100	0.031–31.25 µg/cm^2	neg.	neg.	/					
					MMS	100 µM	neg.	neg.	/					
					$KBrO_3$	2 µM	neg.	neg.	/					
HepaRG	Ultra-low attachment plates (ULA) (96-U-well)	10 days	Viability	ATP assay	MMS	10 µg/ml			neg.					[59]
					CPA	125–1000 µM			neg.					
					ET	0.5–2 µM			2 µM					
					AA	250–2000 µM			neg.					
					2,4-DAT	250–2000 µM			neg.					
					DMBA	5–40 µM			neg.					
					2-AAF	25–200 µM			neg.					
					PhIP	10–320 µM			320 µM					
					IQ	10–320 µM			160 and 320 µM					
					B(a)P	5–20 µM			neg.					
HepaRG	Ultra-low attachment plates (ULA) (96-U-well)	10 days	Viability	ATP assay	4-NQO	0.25–5 µM		5 µM						[73]
					$CdCl_2$	0.1–8 µM		4 µM						
					Cisplatin	1–50 µM		50 µM						
					COL	0.1–40 µM		4 µM						
					ENU	100–3200 µM		2.400 µM						
					ET	2.3–100 µM		100 µM						
					HQ	6.3–200 µM		200 µM						
					MMS	10–500 µM		500 µM						
					2,4-DAT	125–8000 µM		8.000 µM						
					2-AAF	25–400 µM		400 µM						
					AA	156.3–5000 µM		5.000 µM						
					AFB1	0.12–3.75 µM		3.75 µM						
					B(a)P	1–100 µM		100 µM						
					CPA	156.3–10000 µM		5.000 µM						
					DMBA	10–1000 µM		1.000 µM						
					DMNA	7.3–10000 µM		10.000 µM						
					IQ	7.8–375 µM		250 µM						
					PhIP	15.6–750 µM		375 µM						
					Styrene	234.4–10000 µM		10.000 µM						
					3-MCPD	117.2–10000 µM		375 µM						
					DFPBA	7.8–500 µM		100 µM						
					EDAC	1.2–100 µM		750 µM						
					HOPO	11.7–750 µM		1.875 µM						

(*continued on next page*)

Table 3 (*continued*)

Cell line	Method for spheroid formation	Time before treat-ment	End-point	Assay	Chemical/ nanoparticle (NP)/ microplastic (MP) tested	Concentration range	Exposure time/ Effect/LOAEC							R
							30m/ 3h/6h	24 h	48 h	72 h	96 h	120 h	6d/7d/9d/ 14d/21d+	
					PBA	39.1–2500 μM		187.5 μM						
					4-Nitrophenol	3.9–250 μM		10.000 μM						
					Ethyl acrylate	58.6–10000 μM		7.500 μM						
					Phthalic anhydride	117.2–7500 μM		10.000 μM						
					Sodium xylene-sulfonate	117.2–10000 μM		93.8 μM						
					TBHQ	2.9–250 μM		7.500 μM						
					1,4-Dioxane	156.3–10000 μM		1.000 μM						
					Dicyclanil	11.7–1000 μM		500 μM						
					DMTP	11.7–500 μM		5.000 μM						
					Estragole	58.6–5000 μM		500 μM						
HepaRG	Ultra-low attachment plates (ULA) (96-U-well)	10 days	Viability	ATP assay	4-NQO	0.08–10 μM		10 μM						[112]
					$CdCl_2$	0.08–20 μM		X						
					Cisplatin	0.08–40 μM		12.5 μM						
					Colchicine	0.03–2.6 μM		1 μM						
					ENU	32–3200 μM		3200 μM						
					ET	0.25–25 μM		25 μM						
					HQ	3.9–400 μM		300 μM						
					MMS	3.9–500 μM		500 μM						
					2,4-DAT	40–10000 μM		5000 μM						
					2-AAF	12.5–1000 μM		1000 μM						
					AA	78.1–5000 μM		5000 μM						
					AFB1	0.04–2 μM		1 μM						
					B(a)P	0.4–100 μM		100 μM						
					CPA	78–10000 μM		5000 μM						
					DMBA	1.5–500 μM		125 μM						
					NDMA	78–10000 μM		5000 μM						
					IQ	3.9–500 μM		500 μM						
					PhIP	15.6–1000 μM		1000 μM						
					Styrene	100–10000 μM		neg.						
					3-MCPD	70.1–10000 μM		neg.						
					DFPBA	7.8–1000 μM		300 μM						
					EDAC	1.6–300 μM		750 μM						
					HOPO	7.8–800 μM		5000 μM						
					PBA	50–5000 μM		500 μM						
					4-Nitrophenol	5–500 μM		7500 μM						
					Ethyl acrylate	70.1–7500 μM		10000 μM						
					Phthalic anhydride	100–10000 μM		10000 μM						
					Sodium xylene-sulfonate	100–10000 μM		375 μM						
					TBHQ	3.9–375 μM		10000 μM						
					1,4-Dioxane	100–10000 μM		3000 μM						
					Dicyclanil	20–3000 μM		1000 μM						
					DMTP	7.9–1000 μM		neg.						

(*continued on next page*)

Table 3 (*continued*)

Cell line	Method for spheroid formation	Time before treat-ment	End-point	Assay	Chemical/ nanoparticle (NP)/ microplastic (MP) tested	Concentration range	Exposure time/ Effect/LOAEC								R
							30m/ 3h/6h	24 h	48 h	72 h	96 h	120 h	6d/7d/9d/ 14d/21d+		
					Estragole	50–10000 µM		1000 µM							
HepaRG	Ultra-low attachment plates (ULA) (96-U-well)	10 days	viability	ATP assay	CPNP	9.8–1250 µM		neg.							[113]
					NDBA	2–500 µM		neg.							
					NDEA	9.8–1250 µM		neg.							
					NDIPA	9.8–7500 µM		neg.							
					NDMA	7.3–625 µM		neg.							
					NEIPA	9.8–5000 µM		neg.							
					NMBA	9.8–2500 µM		neg.							
					NMPA	2.9–375 µM		neg.							
HepaRG	Ultra-low attachment plates (ULA) (96-U-well)	10 days	Viability	Relative survival (flow cytometry)	NDMA	0.1–2 mM		1 µM	1 µM	0.1 µM					[112]
HepaRG	Ultra-low attachment plates (ULA) (96-U-well)	10 days	Viability	Relative survival (flow cytometry)	CPNP	7.8–4000 µM		4000 µM							[114]
					NDBA	3.9–1500 µM		1500 µM							
					NDEA	19.5–10000 µM		neg.							
					NDIPA	9.8–7500 µM		neg.							
					NDMA	9.8–10000 µM		neg.							
					NEIPA	4.9–5000 µM		2500 µM							
					NMBA	9.8–10000 µM		neg.							
					NMPA	7.8–4000 µM		neg.							
Human primary hepatocytes	Cryopreserved PHH 3D spheroids	7 days	viability	ATP assay	APAP	5–10000 µM			neg.				**7d** 1.100 µM	**14d** 110 µM	[81]
					AFB1	0.001–10 µM			0.5 µM				0.1 µM	0.01 µM	
					Amiodarone	0.5–100 µM			neg.				20 µM	20 µM	
					Chlorpromazine	0.5–100 µM			30 µM				10 µM	8 µM	
					Troglitazone	0.1–100 µM			90 µM				10 µM	2.5 µM	
					Ximelagatran	0.5–1000 µM			neg.				100 µM	40 µM	
Human primary hepatocytes	Ultra-low attachment plates (ULA) (96-U-well) + forced floating	7–10 days	viability	ATP assay	APAP	100–10 000 µM				4.500 µM			**7d** 1.500 µM	**14d** 800 µM	[115]
					Bosentan	4–400 µM				neg.			250 µM	90 µM	
					Diclofenac	5–500 µM				180 µM			100 µM	80 µM	
					Fialuridine	0.3–300 µM				neg.			40 µM	5 µM	
					Pioglitazone	0.4–40 µM				neg.			neg.	neg.	
					Troglitazone	0.4–40 µM				20 µM			15 µM	10 µM	
iPSC derived hepatocytes	Ultra-low attachment plates (ULA) (96-U-well)	4 days	Proliferation	Ki67	MP1	5–100 µg/ml							**6d** neg.	**24d** 5 and 10 µg/ ml	[116]
					MP2	5–100 µg/ml							neg.	5 and 10 µg/ ml	

*neg. -represents no detected effect, /- represents missing data.

**2,4-DAT - 2–4-diaminotoluene; 2-AA- 2-aminoanthracene; 2-AAF- 2-acetylaminofluorene; 3-MCPD - 3-monochloropropane-1,2-diol or 3-chloropropane-1,2-diol; 4-NQO - 4-nitroquinoline N-oxide; AA -acrylamide; AFB1 - Aflatoxin B1; APAP- Acetaminophen; AVA - aminoquinoline; B(a)P - Benzo(a)pyrene; BPA- Bisphenol A; BPAF - Bisphenol AF; BPAP - Bisphenol AP; BPC - Bisphenol C; BPFL - Bisphenol FL; BPS - Bisphenol S; $CdCl_2$ - Cadmium chloride; CHLO - Chlorpromazine hydrochloride; COL - Colchicine; CPA - Cyclophosphamide; CPNP - N-cyclopentyl-4-nitrosopiperazine; CYN - Cylindrospermopsin; DFPBA - (3,5-Diformylphenyl)boronic acid; DMBA - 7,12-dimethylbenz[*a*]anthracene; DMNA - N-Nitrosodimethylamine; DMTP-Dimethylthiophosphate; EDAC-1-Ethyl-3-(3-dimethylaminopropyl)carbodiimide; ENU - N-Nitroso-N-ethylurea; ET - Etoposide; HOPO - 2-Hydroxypyridine-N-oxide; HQ - Hydroquinone; IQ - 2-Amino-3-methyl-3H-imidazo[4,5-*f*]quinoline; KBrO3 - Potassium bromate; MMS - Methyl methanesulfonate; MP1 - Microplastics; MP2- Microplastics; NDBA - N-nitrosodibutylamine; NDEA - N-nitrosodiethylamine; NDIPA - N-nitrosodiisopropylamine; NDMA - N-nitrosodimethylamine; NEIPA - N-nitrosoethylisopropylamine; NMBA - N-nitroso-N-methyl-4-aminobutyric acid; NMPA - N-nitrosomethylphenylamine; NP: CFO - Cobalt ferrite nanoparticle; NP: NFO - Nickel ferrite nanoparticle; NP: TiO2 - Titanium dioxide nanoparticle; NP: Ag - Silver nanoparticle; NP: BaSO4 - Barium sulfate nanoparticle; NP: CeO2 - Ceric oxide nanoparticle; NP: ZFO - Zinc ferrite nanoparticle; NP: FeO - Iron oxide nanoparticle; PBA - Phenylboronic Acid; PhIP - Amino-1-methyl-6-phenylimidazo[4,5-*b*]pyridine; PLN - Piperlongumine; TBHQ - Tert-Butylhydroquinone; Uzara - Extract from Xysmalobium undulatum.

genotoxicity testing, the most frequently used methods to evaluate cell viability in spheroids after exposure to chemicals and nanoparticles were the MTT and MTS assays, the ATP assay, the Alamar Blue and Presto Blue assays, and cell death assessment using the trypan blue assay, while cell proliferation in the spheroids was assessed on a suspension of single cells obtained from spheroids by flow cytometric analyses of the cell cycle and the proliferation marker Ki67, which is expressed only in proliferating cells (Table 3).

HepG2 spheroids have been used to study the impact of direct-acting compounds H_2O_2 [56,101], MMS [56] and etoposide using the comet assay [66]. In addition, Elje et al. [56] used formamidopyrimidine DNA glycosylase (Fpg), an enzyme that detects and excises oxidised and alkylated base lesions, and the results showed that H_2O_2 and MMS-induced increased DNA strand breaks formation in the presence of the Fpg enzyme, suggesting that the enzyme-linked comet assay can be successfully used in 3D cell models [56]. Moreover, the modified comet assay using the Fpg enzyme has also been applied for the detection of DNA strand breaks formed by nanoparticles; however, no effect on the level of DNA damage has been observed after exposure of HepG2 spheroids to non-cytotoxic concentrations of TiO_2-NPs, Ag-NPs, ZnO-NPs without and with Fpg enzyme, corresponding to the results obtained in HepG2 monolayer cultures. The positive control H_2O_2 induced a positive response within the expected range [51].

In the study on HepG2 spheroids developed by the forced floating method, Sendra et al. (2023) [60] reported that six bisphenols (BPA, BPS, BPAP, BPAF, BPFL and BPC), which are metabolically transformed, induced primary DNA damage after 24 and 96 h of exposure. Similar was reported for pro-genotoxic compounds, BaP, AFB1, IQ, and PhIP, which caused DNA damage in HepG2 spheroids after 24-hour exposure detected with the comet assay. In the same study, the sensitivity of HepG2 2D and 3D cell models was compared and the spheroids proved to be more sensitive for detection of indirect-acting genotoxic compounds [66].

The cytokinesis-block micronucleus (CBMN) and mononuclear micronucleus assays were used to study the effects of chemicals and nanoparticles on chromosomal instability. The CBMN is a reliable technique for measuring fixed chromosomal damage in cells that have undergone cell division, which should be considered especially in 3D cell models where cell proliferation is diminished. In HepG2 spheroids developed by hanging drop method, the indirect-acting aflatoxin B1 [61,67] and PhIP [61], as well as direct-acting alkylating agent MMS [67] induced micronuclei formation. The authors reported that AFB1, PhIP and BaP at lower concentrations induced higher MN frequencies in 3D HepG2 spheroids compared to 2D HepG2 monolayer cultures, while direct-acting MMS induced similar levels of MN formation in both 2D and 3D HepG2 models indicating higher metabolic capacity of 3D cell models [61,67]. Moreover, Conway et al. (2020) [67] compared the performance of CBMN assay (addition of CytoB) and mononuclear (MN) micronucleus assay (without addition of CytoB) in HepG2 spheroids after 5 days of exposure to zinc oxide engineered nanomaterials (ZnO ENMs) and reported that after prolonged exposure, when cell proliferation in the 3D conformation is reduced, the CBMN assay underestimated the true level of genotoxicity. They observed a significant difference between the two modifications of the method and reported a clear trend of higher MN frequency due to ZnO ENMs for mononucleated cells. In the same study, HepaRG cells were also used in parallel; however, due to the very low proliferation rate, the authors concluded that HepaRG cells are not suitable for genotoxicity assessment using CBMN assay after long-term exposure of several days unless epidermal growth factors are added to stimulate cell proliferation [113,114]. Llewellyn et al. (2020, 2021) reported that ENMs including TiO_2, ZnO, Ag, $BaSO_4$ and CeO_2 affected chromosomal instability of HepG2 cells in spheroids after 24 h of exposure detected by the CBMN assay, while only ZnO increased the level of micronuclei also after 120 h of exposure detected by the mononucleate version of the micronucleus assay [63,117].

Literature data have shown that the expression of specific genes involved in DNA damage response has been studied mainly in HepG2 and HepG2/C3A spheroids, focusing on the effects of model genotoxic compounds. The key genes investigated in these studies were *TP53*, *CDKN1α*, *MDM2*, *ERCC4* and *GADD45α*. In HepG2 spheroids developed by the forced floating method, BaP and PhIP induced the formation of the DNA double-strand breaks after 24 and 96 h of exposure detected with the γH2AX assay [62], while BPA, BPAP, BPAF and BPC in the same model induced DNA double-strand breaks and pH3-positive cells, reflecting clastogenic and aneugeic effects, respectively [60]. Moreover, in HepG2 spheroids after 72 h of exposure, cylindrospermopsin (CYN), an emerging toxin produced by cyanobacteria that exhibits genotoxic effects in metabolically competent systems caused the increased formation of γH2AX positive foci, reflecting DNA double-strand breaks [41]. For studying the mechanisms of action, a toxicogenomic approach was used in HepG2 spheroids and the results revealed that BaP, AFB1, and two heterocyclic aromatic amines, PhIP and IQ, as well as direct-acting ET, upregulated the mRNA level of genes involved in the response to DNA damage (*TP53*, *CDKN1α*, *GADD45α*) and metabolism (*CYP3A4, CYP1A1, CYP1A2, UGT1A1, SULT1A1, SULT1B1, NAT1, NAT2)* [66]. Similarly, also CYN after 72-hour exposure caused deregulation of genes encoding phase I (*CYP1A1, CYP1A2, CYP3A4, ALDH3A*) and II (*NAT1, NAT2, SULT1B1, SULT1C2, UGT1A1, UGT2B7*) enzymes and genes involved in DNA damage response (*CDKN1α, GADD45α, ERCC4*) [41].

Similar to HepG2 spheroids, the comet assay was the most commonly used method for assessing genotoxic activity also in HepG2/C3A spheroids formed in agreewells and grown in a dynamic Clinostar bioreactor system for 21 days [42] and in cell-repellent microplates and agarose ultra-low attachment plates - agarose liquid overlay technique - cultured for 7 and 10 days [109]. In both systems, indirect-acting BaP and PhIP resulted in an increased formation of DNA single-strand breaks after 24 [42,109] and 96 [42] hours of exposure. In addition, Coltman et al. (2021) [109] reported elevated levels of DNA single-strand breaks induced by pro-genotoxic 2-amino-anthracene (2-AA) and DNA double-strand breaks induced by both indirect-acting (BaP, PhIP, 2-AA) and direct-acting (4-NQO) genotoxic compounds detected with the γH2AX phosphorylation assay. The authors compared HepG2/C3A 3D spheroids and 2D monolayer cultures and concluded that the spheroids are a more sensitive model for detecting pro-genotoxic compounds [109]. The toxicogenomic approach is often used when assessing the mechanisms of action of various compounds. In HepG2/C3A spheroids several genes involved in metabolism (e.g., *CYP1A1, CYP1A2, EPHX, NAT2, UGT1A1, UGT1A3 and UGT1A6, GSTm1, GSTm1, SULT1A1* and *SULT1A2*), cellular stress (e.g., *MKI67, HIF1α, NFKB, NQN1 and NRF2*) and DNA damage response (e.g., *TP53, BRCA2, CDK2, CDK7 and CDKN1α, GADD45α, HUS1, MDM2 and SERTAD1*) were deregulated upon exposure to genotoxic compounds for 24 h [109]. Similar observations were reported by Štampar et al. (2021) [42], when DNA-damage response-related genes (e.g., *TP53, CDKN1α, GADD45α, MDM2 and ERCC4*), immediate-early response genes (*JUNB* and *MYC*) and metabolic genes (e.g., *CYP1A1, CYP1A2, CYP3A4, UGT1A1, UGT2B7, NAT1, NAT2, SULT1B1* as well as *SULT1C2*) were deregulated in 21-old spheroids exposed to BaP and PhIP for 24 h.

In HepaRG spheroids formed in ultra-low attachment plates and cultured for 10 days, the genotoxicity of more than 34 chemicals (including 8 direct-acting and 11 indirect-acting genotoxic compounds or carcinogens and 15 compounds that showed different genotoxic responses *in vitro* and *in vivo*) [73] and 11 chemicals [59] was detected by the CometChip assay and alkaline comet assay, respectively. Both studies revealed that 3D HepaRG spheroids exhibited higher sensitivities than 2D differentiated HepaRG cells and are therefore more suitable to detect DNA damage caused by direct- and indirect-acting genotoxic compounds. Recently, Seo et al. (2024) reported that N-nitrosodimethylamine (NDMA), an alkylating agent metabolized by *CYP2E1*, induced a dose-dependent formation of DNA strand breaks in HepaRG spheroids, which was detected by the alkaline comet assay [112]. Furthermore, genotoxicity of eight *N*-nitrosamines (CPNP, NDBA, NDEA, NDMA, NDIPA, NEIPA, NMBA and NMPA) assessed with the CometChip assay revealed that after 24-hour exposure all tested *N*-nitrosamines caused DNA damage in HepaRG spheroids, while only three (NDBA, NDEA and NDMA) produced positive response in 2D HepaRG cells [114]. In addition to the chemicals, titanium dioxide (TiO_2) and two types of zinc oxide (ZnO) nanoparticles (NMs) were tested for their potential genotoxic activity in the absence and presence of Fpg enzyme in 2D and 3D HepaRG models using both classical and high-throughput (CometChip) formats of the comet assay. The TiO_2 NMs did not show cytotoxic nor genotoxic activities in either the 2D or 3D system. In contrast, the cytotoxic effects of ZnO NMs (ZnO S and NM-110) were greater in the 2D compared to the 3D cell model. ZnO S caused DNA damage only at cytotoxic concentrations, whereas NM-110 showed significant genotoxic effects at non-cytotoxic concentrations in both 2D and 3D models. The positive controls, direct-acting MMS and $KBrO_3$, gave a similar response in the 2D and 3D HepaRG models [93].

In another study on HepaRG spheroids, the results of the micronucleus assay (MN) showed that AFB1 and MMS did not increase the levels of micronuclei after 24 h, which is probably due to low division of HepaRG cells in 3D conformation [67]. The high-throughput (HT) flow-cytometry-based MN assay was adapted for HepaRG spheroids and used to assess genotoxic activity of 34 compounds, including 8 direct-acting compounds, 19 genotoxic or carcinogenic compounds, and 15 compounds that show different genotoxic responses *in vitro* and *in vivo*. The results showed comparable sensitivity of 2D and 3D HepaRG models for direct-acting compounds, however, a much higher sensitivity of 3D HepaRG cells for detection of indirect-acting genotoxic compounds compared to 2D cell cultures was reported, which is likely due to the higher levels of cytochrome P450 (CYP) gene expression and enzyme activities in the spheroids [113]. Five out of eight tested *N*-nitrosamines caused a significant increase in the frequency of MNi in human epidermal growth factor-stimulated 3D HepaRG cell model determined with the flow cytometry-based micronucleus (MN) assay and the sensitivity of the 3D cell model was reported to be higher compared to 2D HepaRG monolayer culture. In addition, all eight nitrosamines induced statistically significant increases in γH2A.X formation in 3D spheroids [114]. In a recent study, Seo et al. (2024) [112] reported that NDMA induced formation of MNi in 2D and 3D HepaRG cell models again with 3D being more sensitive. In addition, the induction of NDMA mutations was studied using two error-corrected next-generation sequencing (ecNGS) technologies (Duplex Sequencing (DS) and High-Fidelity (HiFi) Sequencing) to identify and quantify rare mutations. Mutational spectrum analyses showed predominantly induction of A:T → G:C transitions, along with a lower frequency of G:C → A:T transitions [112].

5. Conclusions

It is becoming increasingly recognized that *in vitro* 3D cell models represent a significant advancement in genotoxicity testing and can contribute to reducing the number of animals used for scientific purposes. Literature data have revealed that 3D hepatic cell models (e.g., HepG2, HepG2/C3A, HepaRG etc.) appear to be more sensitive than 2D monolayer cultures when assessing the genotoxic activities of indirect-acting compounds. As 3D cell models are a physiologically more accurate and ethically more responsible alternative to traditional 2D cell cultures on the one hand and animal experiments on the other hand, increasing the accuracy of toxicity assessments and significantly enhancing the safety of chemicals and public health, it can be concluded that they represent a powerful model for genotoxicity assessment. Since chemicals and nanoparticles can cause genotoxicity by various mechanisms (e.g., primary DNA damage, chromosomal instability, chromosomal aberration, mutations etc.), an integrated test battery measuring different genotoxicity endpoints is warranted to provide information for appropriate follow-up *in vivo* testing, thereby reducing unnecessary animal studies.

Table 4
Studies describing the use of 3D cell models to identify DNA damage caused by chemicals, nanoparticles or natural toxins. The table includes information on the cell model, method of spheroid formation, maturation time, endpoints determined, compounds tested, duration of exposure and effects observed.

Cell line	Method for spheroid formation	Time before treat-ment	End-point Assay	Chemical/ nanoparticle (NP)/ microplastic (MP) tested	Concentration range	Exposure time/ Effect/LOAEC						R
						30min/ 3h/6h	24 h	48 h	72 h	96 h	120 h	
HepG2	Hanging drop	4 days	Comet assay	NP: TiO_2	1–75 µg/cm^2		neg.					[51]
				NP: Ag	1–10 µg/cm^2		neg.					
				NP: ZnO	1–10 µg/cm^2		neg.					
HepG2	Hanging drop	/	Comet assay (CometChip® system)	H_2O_2	10–200 µM	**30 min** 75 µM						[101]
				SIN −1	2–40 mM	**30 min** 2 mM						
HepG2	Hanging drop	4 days + 7 days in 96 well plate	Comet assay	H_2O_2	12.5–250 µM		100 µM					[56]
HepG2	Forced floating (96-U-well)	3 days	Comet assay	BPA	24 h: 1–40 µM; 96 h: 0.1–10 µM		neg.			10 µM		[60]
				BPS	24 h: 1–40 µM; 96 h: 0.1–10 µM		40 µM			1 µM		
				BPAP	24 h: 1–40 µM; 96 h: 0.1–10 µM		40 µM			1 µM		
				BPAF	24 h: 1–40 µM; 96 h: 0.1–10 µM		10 µM			1 µM		
				BPFL	24 h: 1–40 µM; 96 h: 0.1–10 µM		neg.			1 µM		
				BPC	24 h: 1–40 µM; 96 h: 0.1–10 µM		neg.			10 µM		
HepG2	Forced floating (96-U-well)	3 days	Comet assay	B(a)P	10–40 µM		10 µM					[66]
				AFB1	10–40 µM		20 µM					
				PhIP	50–200 µM		50 µM					
				IQ	50–250 µM		100 µM					
				ET	0.17–17 µM		1.7 µM					
HepG2	Hanging drop	3 days	Cytokinesis-block micronucleus (CBMN) (24 h exposure) assay and Micro-nucleus assay (120 h exposure)	NP: TiO_2	0.2–10 µg/ml		2.0 µg/ml				neg.	[63]
				NP: ZnO	0.2–10 µg/ml		0.5 µg/ml				0.2 µg/ ml	
				NP: Ag	0.2–10 µg/ml		0.5 µg/ml				neg.	
				NP: $BaSO_4$	0.2–10 µg/ml		0.2 µg/ml				neg.	
				NP: CeO_2	0.2–10 µg/ml		5.0 µg/ml				neg.	
HepG2	Hanging drop	4 days	Cytokinesis-block micronucleus (CBMN)	NP: TiO_2	5 µg/ml		5 µg/ml					[117]
				NP: Ag	5 µg/ml		neg.					
HepG2	Hanging drop	4 days	Micronucleus assay	NP: TiO_2	5 µg/ml						neg.	[117]
				NP: Ag	5 µg/ml						neg.	
HepG2	Hanging drop	3 days	Micronu-cleus assay	AFB1	0.01–0.2 µM		0.025 µM					[67]
				MMS	5–30 µM		10 µM					
HepG2	Hanging drop	4 days	Micronu-cleus assay	B(a)P	2–8 µM		3 µM					[61]
				PhIP	5–15 µM		5 µM					
HepG2	Hanging drop	4 days	Cytokinesis-block micronucleus (CBMN) assay	Urethane	1.25–50 mM		20 mM					[43]
HepG2	Forced floating (96-U-well)	3 days	Double strand breaks (DBS)-γH2AX	B(a)P	24 h: 0.1–40 µM; 72 h: 0.001–10 µM		1 µM		1 µM			[62]
				PhIP	24 h: 50–200 µM; 72 h: 25–200 µM		200 µM		25 µM			
HepG2	Forced floating (96-U-well)	3 days	Double strand breaks (DBS)-γH2AX	BPA	24 h: 0.1–40 µM; 96 h: 0.01–10 µM		neg.			0.1 µM		[60]
				BPS	24 h: 0.1–40 µM; 96 h: 0.01–10 µM		neg.			neg.		
				BPAP	24 h: 0.1–40 µM;		neg.			neg.		

(*continued on next page*)

Table 4 (*continued*)

Cell line	Method for spheroid formation	Time before treat-ment	End-point Assay	Chemical/ nanoparticle (NP)/ microplastic (MP) tested	Concentration range	Exposure time/ Effect/LOAEC						R
						30min/ 3h/6h	24 h	48 h	72 h	96 h	120 h	
					96 h: 0.01–10 μM							
				BPAF	24 h: 0.1–40 μM; 96 h: 0.01–10 μM		40 μM			10 μM		
				BPFL	24 h: 0.1–40 μM; 96 h: 0.01–10 μM		neg.			neg.		
				BPC	24 h: 0.1–40 μM; 96 h: 0.01–10 μM		40 μM			neg.		
HepG2	Forced floating (96-U-well)	3 days	pH3-mitotic cells	BPA	24 h: 0.1–40 μM; 96 h: 0.01–10 μM		neg.			0.1 μM		[60]
				BPS	24 h: 0.1–40 μM; 96 h: 0.01–10 μM		neg.			neg.		
				BPAP	24 h: 0.1–40 μM; 96 h: 0.01–10 μM		neg.			neg.		
				BPAF	24 h: 0.1–40 μM; 96 h: 0.01–10 μM		40 μM			10 μM		
				BPFL	24 h: 0.1–40 μM; 96 h: 0.01–10 μM		neg.			neg.		
				BPC	24 h: 0.1–40 μM; 96 h: 0.01–10 μM		40 μM			neg.		
HepG2	Forced floating (96-U-well)	3 days	Transcriptomics (selected genes encoding DNA damage responsive genes)	B(a)P	40 μM		↑: *TP53* (1.5-fold), *CDKN1A* (11.4-fold), *GADD45α* (2.93-fold)					[66]
				AFB1	40 μM		↑: *TP53* (1.5-fold), *CDKN1A* (16.6-fold), *GADD45α* (2.1-fold)					
				PhIP	200 μM		No up regulation					
				IQ	250 μM		↑: *CDKN1A* (12.6-fold)					
				ET	17 μM		↑: *MDM2* (1.7-fold), *GADD45α* (3.4-fold)					
HepG2	Forced floating (96-U-well)	3 days	Transcriptomics (DNA damage responsive genes)	CYN	0.5 μg/ml				↑: *CDKN1A* (10.6-fold), *GADD45α* (32.7-fold), *ERCC4* (5.6-fold)			[41]
				B(a)P	30 μM				↑: *CDKN1A* (22.0-fold), *GADD45α* (4.8-fold), *ERCC4* (1.9-fold),			

(*continued on next page*)

Table 4 (*continued*)

Cell line	Method for spheroid formation	Time before treat-ment	End-point Assay	Chemical/ nanoparticle (NP)/ microplastic (MP) tested	Concentration range	Exposure time/ Effect/LOAEC						R
						30min/ 3h/6h	24 h	48 h	72 h	96 h	120 h	
									CCND1 (2.0-fold)			
HepG2/ C3A	Aggrewell + Clinostar	24 h + 21 days	Comet assay	B(a)P	24 h: 40 µM; 96 h: 4 µM		40 µM			4 µM		[42]
				PhIP	24 h: 200, 400 µM; 96 h: 100 µM		200 µM			100 µM		
HepG2/ C3A	Cell-repellent microplates with agarose liquid overlay (LOT)	7 days	Comet assay	B(a)P 2-AA 4-NQO PhIP	3–30 µM 3–30 µM 3–30 µM 3, 10, 30 µM		10 µM neg. 30 µM 10 µM					[109]
HepG2/ C3A	Forced floating (96-U-well)	3 days	Comet assay	PLN	40 µM	**3 h** 40 µM						[98]
HepG2/ C3A	Cell-repellent microplates with agarose liquid overlay (LOT)	7 days	Double strand breaks (DBS)-γH2AX	B(a)P 2-AA 4-NQO PhIP	3–30 µM 3–30 µM 3–30 µM 3–30 µM		10 µM 3 µM 10 µM 3 µM					[109]
HepG2/ C3A	Cell-repellent microplates with agarose liquid overlay (LOT)	7 days	Transcriptomics (targeted DNA damage responsive genes)	B(a)P	30 µM		↑: *BRCA2* (3-fold), *CDK2* (1.7-fold), *CDK7* (2.2-fold), *CDKN1A* (45.8-fold), *GADD45α* (15-fold), *HUS1* (2.5-fold), *MDM2* (2.9-fold), *SERTAD1* (9.3-fold)					[109]
				2-AA 4-NQO	30 µM 30 µM		neg. ↑: *CDKN1A* (>5-fold); *GADD45α* (>2-fold), *SERTAD1* (>1.5-fold)					
				PhIP	30 µM		↑: *CDKN1A* (>2-fold)					
HepG2/ C3A	Forced floating (96-U-well)	3 days	Transcriptomics (DNA damage responsive genes)	PLN	40 µM		↑: *CDKN1A* (4.8-fold), *GADD45α* (1.6-fold), *H2AFX* (1.5-fold), *MDM2* (3-fold)					[98]
HepG2/ C3A	Aggrewell + Clinostar	24 h + 21 days	Transcriptomics (DNA damage responsive genes)	B(a)P	24 h: 40 µM; 96 h: 4 µM		↑: *TP53* (1.8-fold), *CDKN1A* (29.5-fold), *GADD45α* (13.5-fold), MDM2 (1.9-fold), ERCC4 (3.3-fold)		↑: *TP53* (2.9-fold), *CDKN1A* (46.5-fold), *GADD45α* (10.4-fold), *MDM2* (3.7-fold), *ERCC4* (3.2-fold)			[42]
				PhIP	24 h: 400 µM; 96 h: 100 µM		↑: *CDKN1A1* (3.8-fold), *MDM2* (1.71-fold), *ERCC4* (2.0-fold)		neg.			

(*continued on next page*)

Table 4 (*continued*)

Cell line	Method for spheroid formation	Time before treat-ment	End-point Assay	Chemical/ nanoparticle (NP)/ microplastic (MP) tested	Concentration range	Exposure time/ Effect/LOAEC						R
						30min/ 3h/6h	24 h	48 h	72 h	96 h	120 h	
HepaRG	Ultra-low attachment plates (ULA) (96-U-well)	10 days	comet assay (CometChip® system)	4-NQO	0.25–5 µM		1.88 µM					[73]
				$CdCl_2$	0.1–8 µM		3 µM					
				Cisplatin	1–50 µM		25 µM					
				COL	0.1–40 µM		neg.					
				ENU	100–3200 µM		1.600 µM					
				ET	2.3–100 µM		50 µM					
				HQ	6.3–200 µM		neg.					
				MMS	10–500 µM		80 µM					
				2,4-DAT	125–8000 µM		6.000 µM					
				2-AAF	25–400 µM		neg.					
				AA	156.3–5000 µM		937.5 µM					
				AFB1	0.12–3.75 µM		neg.					
				B(a)P	1–100 µM		25 µM					
				CPA	156.3–10000 µM		1.250 µM					
				DMBA	10–1000 µM		750 µM					
				DMNA	7.3–10000 µM		78.1 µM					
				IQ	7.8–375 µM		187.5 µM					
				PhIP	15.6–750 µM		187.5 µM					
				Styrene	234.4–10000 µM		neg.					
				3-MCPD	117.2–10000 µM		7.500 µM					
				DFPBA	7.8–500 µM		neg.					
				EDAC	1.2–100 µM		neg.					
				HOPO	11.7–750 µM		neg.					
				PBA	39.1–2500 µM		neg.					
				4-Nitrophenol	3.9–250 µM		neg.					
				Ethyl acrylate	58.6–10.000 µM		neg.					
				Phthalic anhydride	117.2–7500 µM		neg.					
				Sodium xylene-sulfonate	117.2–10.000 µM		neg.					
				TBHQ	2.9–250 µM		neg.					
				1,4-Dioxane	156.3–10.000 µM		neg.					
				Dicyclanil	11.7–1000 µM		neg.					
				DMTP	11.7–500 µM		neg.					
				Estragole	58.6–5000 µM		neg.					
				LMG	5.9–500 µM		neg.					
HepaRG	Ultra-low attachment plates (ULA) (96-U-well)	10 days	Comet assay	MMS	9–90 µg/ml		45 µM					[59]
				CPA	125–1000 µM		1000 µM					
				4-NQO	0.0675–0.500 µM		0.25 µM					
				ET	0.5–2 µM		neg.					
				AA	250–2000 µM		500 µM					
				2,4-DAT	250–2000 µM		neg.					
				DMBA	5–40 µM		20 µM					
				2-AAF	25–200 µM		50 µM					
				PhIP	10–320 µM		40 µM					
				IQ	10–320 µM		neg.					
				B(a)P	5–20 µM		20 µM					
HepaRG	Ultra-low attachment plates (ULA) (96-U-well)	10 days	Comet assay	NDMA	0.1–2 mM				0.1 mM			[112]
HepaRG	Ultra-low attachment plates (ULA) (96-U-well)	8 days	Comet assay (CometChip® system)	NP: TiO_2	0.31–31.25 µg/ cm^2		/	neg.				[93]
				NP: ZnO S	0.031–31.25 µg/cm^2		7.8125 µg/ cm^2	/				
				NP: ZnO NM−110	0.031–31.25 µg/cm^2		7.8125 µg/ cm^2	/				
				MMS	100 µM		100 µM	/				
				KBrO3	2 µM		2 µM	/				
HepaRG	Ultra-low attachment plates (ULA) (96-U-well)	10 days	Comet assay (CometChip® system)	CPNP	9.8–1250 µM		312.5 µM					[114]
				NDMA	2–500 µM		125 µM					
				NDEA	9.8–1250 µM		312.5 µM					
				NDIPA	9.8–7500 µM		5000 µM					

(*continued on next page*)

Table 4 (*continued*)

Cell line	Method for spheroid formation	Time before treat-ment	End-point Assay	Chemical/ nanoparticle (NP)/ microplastic (MP) tested	Concentration range	Exposure time/ Effect/LOAEC						R
						30min/ 3h/6h	24 h	48 h	72 h	96 h	120 h	
				NDMA	7.3–625 µM		312.5 µM					
				NEIPA	9.8–5000 µM		2500 µM					
				NMBA	9.8–2500 µM		625 µM					
				NMPA	2.9–375 µM		187.5 µM					
HepaRG	Ultra-low attachment plates (ULA) (96-U-well)	10 days	Micronucleus assay (high-throughput (HT) flow-cytometry-based MN assay + stimulation of cell division with human epidermal growth factors)	NDMA	0.1–2 mM				0.5 mM			[112]
HepaRG	Ultra-low attachment plates (ULA) (96-U-well)	10 days	Micronucleus assay (high-throughput (HT) flow-cytometry-based MN assay + stimulation of cell division with human epidermal growth factors)	4-NQO	0.08–10 µM		2 µM					[113]
				$CdCl_2$	0.08–20 µM		neg.					
				Cisplatin	0.08–40 µM		10 µM					
				Colchicine	0.03–2.6 µM		0.5 µM					
				ENU	32–3200 µM		2400 µM					
				ET	0.25–25 µM		10 µM					
				HQ	3.9–400 µM		neg.					
				MMS	3.9–500 µM		500 µM					
				2,4-DAT	40–10,000 µM		neg.					
				2-AAF	12.5–1000 µM		800 µM					
				AA	78.1–5000 µM		neg.					
				AFB1	0.04–2 µM		0.31 µM					
				B(a)P	0.4–100 µM		40 µM					
				CPA	78–10,000 µM		2500 µM					
				DMBA	1.5–500 µM		7.8 µM					
				DMNA	78–10,000 µM		2500 µM					
				IQ	3.9–500 µM		neg.					
				PhIP	15.6–1000 µM		1000 µM					
				Styrene	100–10000 µM		neg.					
				3-MCPD	70.1–10000 µM		neg.					
				DFPBA	7.8–1000 µM		neg.					
				EDAC	1.6–300 µM		neg.					
				HOPO	7.8–800 µM		neg.					
				PBA	50–5000 µM		neg.					
				4-Nitrophenol	5–500 µM		neg.					
				Ethyl acrylate	70.1–7500 µM		neg.					
				Phthalic anhydride	100–10,000 µM		neg.					
				Sodium xylene-sulfonate	100–10,000 µM		neg.					
				TBHQ	3.9–375 µM		neg.					
				1,4-Dioxane	100–10,000 µM		neg.					
				Dicyclanil	20–3000 µM		neg.					
				DMTP	7.9–1000 µM		neg.					
				Estragole	50–10,000 µM		neg.					
				LMG	5–1000 µM		neg.					
HepaRG	Ultra-low attachment plates (ULA) (96-U-well)	10 days	Micronucleus assay (high-throughput (HT) flow-cytometry-based MN assay + stimulation of cell division with human epidermal growth factors)	CPNP	7.8–4000 µM		neg.					[114]
				NDBA	3.9–1500 µM		500 µM					
				NDEA	19.5–10,000 µM		5000 µM					
				NDIPA	9.8–7500 µM		neg.					
				NDMA	9.8–10,000 µM		neg.					
				NEIPA	4.9–5000 µM		1250 µM					
				NMBA	9.8–10,000 µM		7500 µM					
				NMPA	7.8–4000 µM		3000 µM					

*neg. -represents no detected effect, /- represents missing data.

**2,4-DAT - 2–4-diaminotoluene; 2-AA - 2-aminoanthracene; 2-AAF - 2-acetylaminofluorene; 3-MCPD - 3-monochloropropane-1,2-diol or 3-chloropropane-1,2-diol; 4-NQO - 4-nitroquinoline N-oxide; AA – Acrylamide; AFB1 - Aflatoxin B1; B(a)P - Benzo(a)pyrene; BPA - Bisphenol A; BPAF - Bisphenol AF; BPAP - Bisphenol AP; BPC - Bisphenol C; BPFL - Bisphenol FL; BPS - Bisphenol S; $CdCl_2$ - Cadmium chloride; COL – Colchicine; CPA – Cyclophosphamide; CPNP - N-cyclopentyl-4-nitrosopiperazine; CYN – Cylindrospermopsin; DFPBA - (3,5-Diformylphenyl)boronic acid; DMBA - 7,12-dimethylbenz[*a*]anthracene; DMNA - N-Nitrosodimethylamine; DMTP – Dimethylthiophosphate; EDAC - 1-Ethyl-3-(3-dimethylaminopropyl)carbodiimide; ENU - N-Nitroso-N-ethylurea; ET – Etoposide; H_2O_2 - Hydrogen peroxide; HOPO - 2-Hydroxypyridine-N-oxide; HQ – Hydroquinone; IQ - 2-Amino-3-methyl-3H-imidazo[4,5-*f*]quinoline; $KBrO_3$ - Potassium bromate; LMG - Leucomalachite Green; MMS - Methyl methanesulfonate; NDBA - N-nitrosodibutylamine; NDEA - N-nitrosodiethylamine; NDIPA - N-nitrosodiisopropylamine; NDMA - N-nitrosodimethylamine; NEIPA - N-nitrosoethylisopropylamine, NMBA - N-nitroso-N-methyl-4-aminobutyric acid; NMPA - N-nitrosomethylphenylamine; NP: Ag – Silver nanoparticle; NP: BaSO4 - Barium sulfate nanoparticle; NP: CeO2 - ceric oxide nanoparticle; NP: TiO2 - Titanium dioxide nanoparticle; NP: ZnO - Zinc oxide nanoparticle; PBA - Phenylboronic Acid; PhIP - Amino-1-methyl-6-phenylimidazo[4,5-*b*]pyridine; PLN - alkaloid Piperlongumine; SIN –1–3-Morpholinosydnonimine hydrochloride; TBHQ - Tert-Butylhydroquinone.

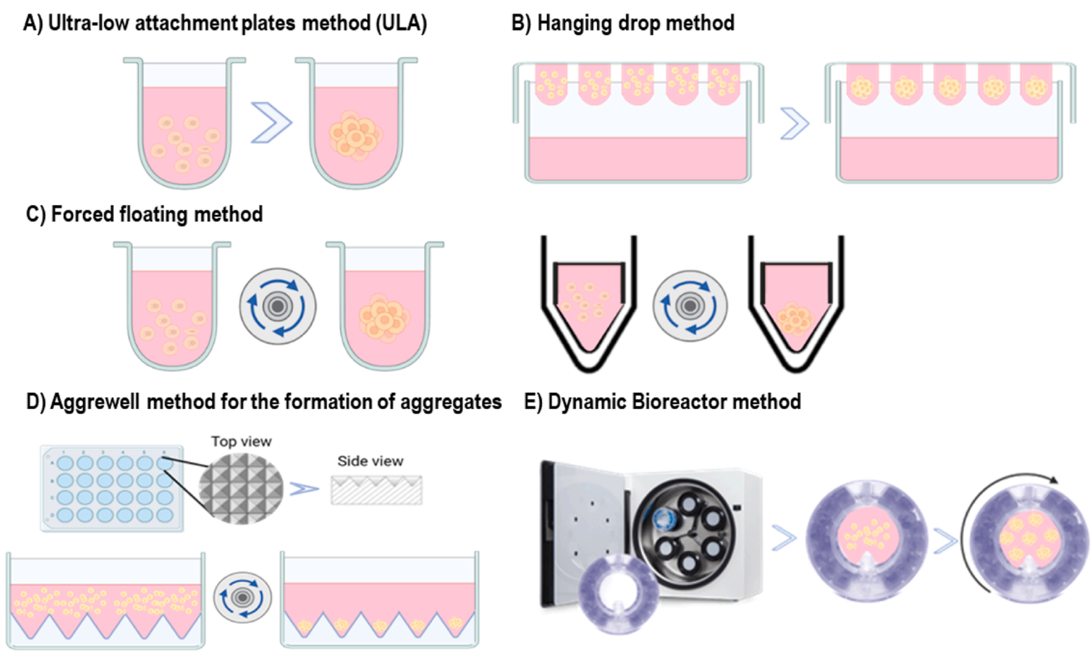

Figure 1. Schematic presentation of the most frequently applied techniques for the formation of spheroids used for genotoxicity assessment (Created with BioRender).

Funding

The study received financial support by Slovenian Research Agency [P1–0245, J1–2465, Z1–3191, J1–4395, BI-BA/24–25–017] and European Union H2020-MSCA NESTOR project (101007629) and HEU Cut-Cancer project (101079113).

CRediT authorship contribution statement

Martina Štampar: Writing – original draft, Methodology, Investigation, Formal analysis, Data curation, Conceptualization. **Bojana Žegura:** Writing – original draft, Resources, Funding acquisition, Formal analysis, Data curation, Conceptualization.

Declaration of Competing Interest

The authors declare that they have no known competing financial interests or personal relationships that could have appeared to influence the work reported in this paper. The authors declare that they do not have any affiliations that would lead to conflicts of interest.

Data Availability

Data will be made available on request.

References

[1] S.C. DeVito, The need for, and the role of the toxicological chemist in the design of safer chemicals, Toxicol. Sci. 161 (2018) 225–240, https://doi.org/10.1093/toxsci/kfx197.
[2] D.E. Buttke, Toxicology, environmental health, and the "One Health" concept, J. Med. Toxicol. 7 (2011) 329–332, https://doi.org/10.1007/s13181-011-0172-4.
[3] L.D. Claxton, G. de A. Umbuzeiro, D.M. DeMarini, The *Salmonella* mutagenicity assay: the stethoscope of genetic toxicology for the 21st century, Environ. Health Perspect. 118 (2010) 1515–1522, https://doi.org/10.1289/ehp.1002336.
[4] R. Corvi, F. Madia, In vitro genotoxicity testingeCan the performance be enhanced?-NC-ND license (http://creativecommons.org/licenses/by-nc-nd/4.0/), Food Chem. Toxicol. 106 (2017) 600–608, https://doi.org/10.1016/j.fct.2016.08.024.
[5] O. Altindag, M. Karakoc, A. Kocyigit, H. Celik, N. Soran, Increased DNA damage and oxidative stress in patients with rheumatoid arthritis, Clin. Biochem. 40 (2007) 167–171, https://doi.org/10.1016/j.clinbiochem.2006.10.006.
[6] J.H.J. Hoeijmakers, DNA damage, aging, and cancer, N. Engl. J. Med. 361 (2009) 1475–1485, https://doi.org/10.1056/NEJMra0804615.
[7] R. Corvi, F. Madia, In vitro genotoxicity testing–Can the performance be enhanced? Food Chem. Toxicol. 106 (2017) 600–608, https://doi.org/10.1016/j.fct.2016.08.024.
[8] M.N. Jacobs, A. Colacci, R. Corvi, M. Vaccari, M.C. Aguila, M. Corvaro, N. Delrue, D. Desaulniers, N. Ertych, A. Jacobs, M. Luijten, F. Madia, A. Nishikawa, K. Ogawa, K. Ohmori, M. Paparella, A.K. Sharma, P. Vasseur, Chemical carcinogen safety testing: OECD expert group international consensus on the development of an integrated approach for the testing and assessment of chemical non-genotoxic carcinogens, Arch. Toxicol. 94 (2020) 2899–2923, https://doi.org/10.1007/s00204-020-02784-5.
[9] EFSA, PUBLIC CONSULTATION DRAFT opinion on genotoxicity testing strategies ENDORSED FOR PUBLIC CONSULTATION DRAFT SCIENTIFIC OPINION, (2011). ⟨www.efsa.europa.eu⟩ (accessed June 22, 2021).
[10] W.S. Stokes, Animals and the 3Rs in toxicology research and testing, Hum. Exp. Toxicol. 34 (2015) 1297–1303, https://doi.org/10.1177/0960327115598410.
[11] P. Fowler, R. Smith, K. Smith, J. Young, L. Jeffrey, D. Kirkland, S. Pfuhler, P. Carmichael, Reduction of misleading (" false") positive results in mammalian cell genotoxicity assays. II. Importance of accurate toxicity measurement, Mutat. Res. - Genet. Toxicol. Environ. Mutagen. 747 (2012) 104–117, https://doi.org/10.1016/j.mrgentox.2012.04.013.
[12] C. Watson, J. Ge, J. Cohen, G. Pyrgiotakis, B.P. Engelward, P. Demokritou, High-throughput screening platform for engineered nanoparticle-mediated genotoxicity using cometchip technology, ACS Nano 8 (2014) 2118–2133, https://doi.org/10.1021/nn404871p.
[13] R.C. Fry, J. Bangma, J. Szilagyi, J.E. Rager, Developing novel in vitro methods for the risk assessment of developmental and placental toxicants in the environment, Toxicol. Appl. Pharmacol. 378 (2019) 114635, https://doi.org/10.1016/j.taap.2019.114635.
[14] H. Wang, T. Xu, D. Yin, Emerging trends in the methodology of environmental toxicology: 3D cell culture and its applications, Sci. Total Environ. 857 (2023) 159501, https://doi.org/10.1016/j.scitotenv.2022.159501.

[15] R.J. Silva, S. Tamburic, A state-of-the-art review on the alternatives to animal testing for the safety assessment of cosmetics, Cosmetics 9 (2022) 90, https://doi.org/10.3390/cosmetics9050090.
[16] A.K. Kiani, D. Pheby, G. Henehan, R. Brown, P. Sieving, P. Sykora, R. Marks, B. Falsini, N. Capodicasa, S. Miertus, L. Lorusso, D. Dondossola, G.M. Tartaglia, M.C. Ergoren, M. Dundar, S. Michelini, D. Malacarne, G. Bonetti, A. Dautaj, K. Donato, M.C. Medori, T. Beccari, M. Samaja, S.T. Connelly, D. Martin, A. Morresi, A. Bacu, K.L. Herbst, M. Kapustin, L. Stuppia, L. Lumer, G. Farronato, M. Bertelli, Ethical considerations regarding animal experimentation, J. Prev. Med. Hyg. 63 (2022) E255–E266, https://doi.org/10.15167/2421-4248/jpmh2022.63.2S3.2768.
[17] A. Astashkina, D.W. Grainger, Critical analysis of 3-D organoid in vitro cell culture models for high-throughput drug candidate toxicity assessments, Adv. Drug Deliv. Rev. 69–70 (2014) 1–18, https://doi.org/10.1016/j.addr.2014.02.008.
[18] H. Olson, G. Betton, D. Robinson, K. Thomas, A. Monro, G. Kolaja, P. Lilly, J. Sanders, G. Sipes, W. Bracken, M. Dorato, K. Van Deun, P. Smith, B. Berger, A. Heller, Concordance of the toxicity of pharmaceuticals in humans and in animals, Regul. Toxicol. Pharmacol. 32 (2000) 56–67, https://doi.org/10.1006/rtph.2000.1399.
[19] N. Shanks, R. Greek, J. Greek, Are animal models predictive for humans? Philos. Ethics, Humanit. Med. 4 (2009) 2, https://doi.org/10.1186/1747-5341-4-2.
[20] D. Kirkland, S. Pfuhler, D. Tweats, M. Aardema, R. Corvi, F. Darroudi, A. Elhajouji, H. Glatt, P. Hastwell, M. Hayashi, P. Kasper, S. Kirchner, A. Lynch, D. Marzin, D. Maurici, J.-R. Meunier, L. Müller, G. Nohynek, J. Parry, E. Parry, V. Thybaud, R. Tice, J. van Benthem, P. Vanparys, P. White, How to reduce false positive results when undertaking in vitro genotoxicity testing and thus avoid unnecessary follow-up animal tests: report of an ECVAM Workshop, Mutat. Res. Toxicol. Environ. Mutagen. 628 (2007) 31–55, https://doi.org/10.1016/J.MRGENTOX.2006.11.008.
[21] S. Cho, J.-Y. Yoon, Organ-on-a-chip for assessing environmental toxicants, Curr. Opin. Biotechnol. 45 (2017) 34–42, https://doi.org/10.1016/j.copbio.2016.11.019.
[22] S. Silvani, M. Figliuzzi, A. Remuzzi, Toxicological evaluation of airborne particulate matter. Are cell culture technologies ready to replace animal testing? J. Appl. Toxicol. 39 (2019) 1484–1491, https://doi.org/10.1002/jat.3804.
[23] N. Burden, K. Chapman, F. Sewell, V. Robinson, Pioneering better science through the 3Rs: an introduction to the National Centre for the Replacement, Refinement, and Reduction of Animals in Research (NC3Rs), J. Am. Assoc. Lab. Anim. Sci. 54 (2015) 198–208. ⟨https://www.ingentaconnect.com/content/aalas/jaalas/2015/00000054/00000002/art00012⟩. accessed January 15, 2020.
[24] L.M. Schechtman, Implementation of the 3Rs (Refinement, Reduction, and Replacement): validation and regulatory acceptance considerations for alternative toxicological test methods, ILAR J. 43 (2002) S85–S94, https://doi.org/10.1093/ilar.43.suppl_1.s85.
[25] A.L. Nagy, C. Catoi, C. Socaciu, A. Pintea, N.A. Oros, C. Coman, D. Rugina, C. T. Matea, T. Mocan, T. Coccini, U. De Simone, I. De Angelis, A. Bertero, Y. Sambuy, F. Caloni, From 3Rs to 3D: in vitro alternative models for replacement, ALTEX 35 (2018) 420–421, https://doi.org/10.14573/altex.1804041.
[26] S. Pfuhler, J. van Benthem, R. Curren, S.H. Doak, M. Dusinska, M. Hayashi, R. H. Heflich, D. Kidd, D. Kirkland, Y. Luan, G. Ouedraogo, K. Reisinger, T. Sofuni, F. van Acker, Y. Yang, R. Corvi, Use of in vitro 3D tissue models in genotoxicity testing: Strategic fit, validation status and way forward. Report of the working group from the 7th International Workshop on Genotoxicity Testing (IWGT), Mutat. Res. Toxicol. Environ. Mutagen. 850–851 (2020) 503135, https://doi.org/10.1016/j.mrgentox.2020.503135.
[27] M. Waldherr, M. Mišík, F. Ferk, J. Tomc, B. Žegura, M. Filipič, W. Mikulits, S. Mai, O. Haas, W.W. Huber, E. Haslinger, S. Knasmüller, Use of HuH6 and other human-derived hepatoma lines for the detection of genotoxins: a new hope for laboratory animals? Arch. Toxicol. 92 (2018) 921–934, https://doi.org/10.1007/s00204-017-2109-4.
[28] OECD (2019), Test No. 431: In vitro skin corrosion: reconstructed human epidermis (RHE) test method, OECD, 2019. https://doi.org/10.1787/9789264264618-en.
[29] OECD, Test No. 487: In Vitro Mammalian Cell Micronucleus Test, OECD Guidelines for the Testing of Chemicals, Section 4, (2023). https://doi.org/10.1787/9789264264861-en.
[30] S. İpek, A. Üstündağ, B. Can Eke, Three-dimensional (3D) cell culture studies: a review of the field of toxicology, Drug Chem. Toxicol. 46 (2023) 523–533, https://doi.org/10.1080/01480545.2022.2066114.
[31] S. Yang, M. Ooka, R.J. Margolis, M. Xia, Liver three-dimensional cellular models for high-throughput chemical testing, Cell Rep. Methods 3 (2023) 100432, https://doi.org/10.1016/j.crmeth.2023.100432.
[32] K.E. Chapman, U.-K. Shah, J.F. Fletcher, G.E. Johnson, S.H. Doak, G.J.S. Jenkins, An integrated in vitro carcinogenicity test that distinguishes between genotoxic carcinogens, non-genotoxic carcinogens, and non-carcinogens, Mutagenesis 39 (2024) 69–77, https://doi.org/10.1093/mutage/geae004.
[33] C. Rowe, D.T. Gerrard, R. Jenkins, A. Berry, K. Durkin, L. Sundstrom, C. E. Goldring, B.K. Park, N.R. Kitteringham, K.P. Hanley, N.A. Hanley, Proteome-wide analyses of human hepatocytes during differentiation and dedifferentiation, Hepatology 58 (2013) 799–809, https://doi.org/10.1002/hep.26414.
[34] M. Baxter, S. Withey, S. Harrison, C.-P. Segeritz, F. Zhang, R. Atkinson-Dell, C. Rowe, D.T. Gerrard, R. Sison-Young, R. Jenkins, J. Henry, A.A. Berry, L. Mohamet, M. Best, S.W. Fenwick, H. Malik, N.R. Kitteringham, C.E. Goldring, K. Piper Hanley, L. Vallier, N.A. Hanley, Phenotypic and functional analyses show stem cell-derived hepatocyte-like cells better mimic fetal rather than adult hepatocytes, J. Hepatol. 62 (2015) 581–589, https://doi.org/10.1016/j.jhep.2014.10.016.
[35] E.L. LeCluyse, Human hepatocyte culture systems for the in vitro evaluation of cytochrome P450 expression and regulation, Eur. J. Pharm. Sci. 13 (2001) 343–368, https://doi.org/10.1016/S0928-0987(01)00135-X.
[36] P. Godoy, N.J. Hewitt, U. Albrecht, M.E. Andersen, N. Ansari, S. Bhattacharya, J. G. Bode, J. Bolleyn, C. Borner, J. Böttger, A. Braeuning, R.A. Budinsky, B. Burkhardt, N.R. Cameron, G. Camussi, C.S. Cho, Y.J. Choi, J. Craig Rowlands, U. Dahmen, G. Damm, O. Dirsch, M.T. Donato, J. Dong, S. Dooley, D. Drasdo, R. Eakins, K.S. Ferreira, V. Fonsato, J. Fraczek, R. Gebhardt, A. Gibson, M. Glanemann, C.E.P. Goldring, M.J. Gómez-Lechón, G.M.M. Groothuis, L. Gustavsson, C. Guyot, D. Hallifax, S. Hammad, A. Hayward, D. Häussinger, C. Hellerbrand, P. Hewitt, S. Hoehme, H.G. Holzhütter, J.B. Houston, J. Hrach, K. Ito, H. Jaeschke, V. Keitel, J.M. Kelm, B. Kevin Park, C. Kordes, G.A. Kullak-Ublick, E.L. Lecluyse, P. Lu, J. Luebke-Wheeler, A. Lutz, D.J. Maltman, M. Matz-Soja, P. McMullen, I. Merfort, S. Messner, C. Meyer, J. Mwinyi, D.J. Naisbitt, A. K. Nussler, P. Olinga, F. Pampaloni, J. Pi, L. Pluta, S.A. Przyborski, A. Ramachandran, V. Rogiers, C. Rowe, C. Schelcher, K. Schmich, M. Schwarz, B. Singh, E.H.K. Stelzer, B. Stieger, R. Stöber, Y. Sugiyama, C. Tetta, W.E. Thasler, T. Vanhaecke, M. Vinken, T.S. Weiss, A. Widera, C.G. Woods, J.J. Xu, K. M. Yarborough, J.G. Hengstler, Recent advances in 2D and 3D in vitro systems using primary hepatocytes, alternative hepatocyte sources and non-parenchymal liver cells and their use in investigating mechanisms of hepatotoxicity, cell signaling and ADME, Arch. Toxicol. 87 (2013) 1315–1530, https://doi.org/10.1007/s00204-013-1078-5.
[37] M. Gomez-Lechon, M. Donato, J. Castell, R. Jover, Human hepatocytes in primary culture: the choice to investigate drug metabolism in man, Curr. Drug Metab. 5 (2004) 443–462, https://doi.org/10.2174/1389200043335414.
[38] S.P. den Braver-Sewradj, M.W. den Braver, N.P.E. Vermeulen, J.N. M. Commandeur, L. Richert, J.C. Vos, Inter-donor variability of phase I/phase II metabolism of three reference drugs in cryopreserved primary human hepatocytes in suspension and monolayer, Toxicol Vitr. 33 (2016) 71–79, https://doi.org/10.1016/j.tiv.2016.02.013.
[39] S.J. Fey, K. Wrzesinski, Determination of drug toxicity using 3D spheroids constructed from an immortal human hepatocyte cell line, Toxicol. Sci. 127 (2012) 403–411, https://doi.org/10.1093/toxsci/kfs122.
[40] L.Le Hégarat, A. Mourot, S. Huet, L. Vasseur, S. Camus, C. Chesné, V. Fessard, Performance of comet and micronucleus assays in metabolic competent HepaRG cells to predict in vivo genotoxicity, Toxicol. Sci. 138 (2014) 300–309, https://doi.org/10.1093/toxsci/kfu004.
[41] K. Hercog, M. Štampar, A. Štern, M. Filipič, B. Žegura, Application of advanced HepG2 3D cell model for studying genotoxic activity of cyanobacterial toxin cylindrospermopsin, Environ. Pollut. 265 (2020) 114965, https://doi.org/10.1016/j.envpol.2020.114965.
[42] M. Štampar, H. Sedighi Frandsen, A. Rogowska-Wrzesinska, K. Wrzesinski, M. Filipič, B. Žegura, Hepatocellular carcinoma (HepG2/C3A) cell-based 3D model for genotoxicity testing of chemicals, Sci. Total Environ. 755 (2021) 143255, https://doi.org/10.1016/j.scitotenv.2020.143255.
[43] U.-K. Shah, J.R. Verma, K.E. Chapman, E.C. Wilde, J.A. Tonkin, M.R. Brown, G. E. Johnson, S.H. Doak, G.J. Jenkins, Detection of urethane-induced genotoxicity in vitro using metabolically competent human 2D and 3D spheroid culture models, Mutagenesis 35 (2020) 445–452, https://doi.org/10.1093/mutage/geaa029.
[44] J. Tang, J. Shi, J. Liu, Editorial: advances in 3D cell culture for drug screening and toxicology evaluation, Front. Bioeng. Biotechnol. 11 (2023), https://doi.org/10.3389/fbioe.2023.1266506.
[45] R. Xie, V. Pal, Y. Yu, X. Lu, M. Gao, S. Liang, M. Huang, W. Peng, I.T. Ozbolat, A comprehensive review on 3D tissue models: biofabrication technologies and preclinical applications, Biomaterials 304 (2024) 122408, https://doi.org/10.1016/j.biomaterials.2023.122408.
[46] V. Brancato, J.M. Oliveira, V.M. Correlo, R.L. Reis, S.C. Kundu, Could 3D models of cancer enhance drug screening? Biomaterials 232 (2020) 119744 https://doi.org/10.1016/j.biomaterials.2019.119744.
[47] G.A. Truskey, Human microphysiological systems and organoids as in vitro models for toxicological studies, Front. Public Heal. 6 (2018), https://doi.org/10.3389/fpubh.2018.00185.
[48] A.L. Caipa Garcia, V.M. Arlt, D.H. Phillips, Organoids for toxicology and genetic toxicology: applications with drugs and prospects for environmental carcinogenesis, Mutagenesis 37 (2022) 143–154, https://doi.org/10.1093/mutage/geab023.
[49] K. Białkowska, P. Komorowski, M. Bryszewska, K. Miłowska, Spheroids as a type of three-dimensional cell cultures—examples of methods of preparation and the most important application, Int. J. Mol. Sci. 21 (2020) 1–17, https://doi.org/10.3390/ijms21176225.
[50] M. Dusinska, A.R. Collins, The comet assay in human biomonitoring: gene-environment interactions, Mutagenesis 23 (2008) 191–205, https://doi.org/10.1093/mutage/gen007.
[51] E. Elje, E. Mariussen, O.H. Moriones, N.G. Bastús, V. Puntes, Y. Kohl, M. Dusinska, E. Rundén-Pran, Hepato(Geno)toxicity assessment of nanoparticles in a HepG2 liver spheroid model, Nanomaterials 10 (2020) 545, https://doi.org/10.3390/nano10030545.
[52] F. Pampaloni, H.K.Stelzer Ernst, Three-dimensional cell cultures in toxicology, Biotechnol. Genet. Eng. Rev. 26 (2009) 117–138, https://doi.org/10.5661/bger-26-117org/10.5661/bger-26-117.

[53] S.C. Ramaiahgari, M.W. Den Braver, B. Herpers, V. Terpstra, J.N. M. Commandeur, B. Van De Water, L.S. Price, A 3D in vitro model of differentiated HepG2 cell spheroids with improved liver-like properties for repeated dose high-throughput toxicity studies, Arch. Toxicol. 88 (2014) 1083–1095, https://doi.org/10.1007/s00204-014-1215-9.

[54] S.V. Llewellyn, A. Kermanizadeh, V. Ude, N.R. Jacobsen, G.E. Conway, U.-K. Shah, M. Niemeijer, M.J. Moné, B. van de Water, S. Roy, W. Moritz, V. Stone, G.J.S. Jenkins, S.H. Doak, Assessing the transferability and reproducibility of 3D in vitro liver models from primary human multi-cellular microtissues to cell-line based HepG2 spheroids, Toxicol. Vitr. 85 (2022) 105473, https://doi.org/10.1016/j.tiv.2022.105473.

[55] M. Štampar, B. Breznik, M. Filipič, B. Žegura, Characterization of in vitro 3d cell model developed from human hepatocellular carcinoma (HepG2) cell line, Cells 9 (2020) 2557, https://doi.org/10.3390/cells9122557.

[56] E. Elje, M. Hesler, E. Rundén-Pran, P. Mann, E. Mariussen, S. Wagner, M. Dusinska, Y. Kohl, The comet assay applied to HepG2 liver spheroids, Mutat. Res. - Genet. Toxicol. Environ. Mutagen. 845 (2019) 403033, https://doi.org/10.1016/j.mrgentox.2019.03.006.

[57] J. Dilz, I. Auge, K. Groeneveld, S. Reuter, R. Mrowka, A proof-of-concept assay for quantitative and optical assessment of drug-induced toxicity in renal organoids, Sci. Rep. 13 (2023) 6167, https://doi.org/10.1038/s41598-023-33110-5.

[58] F. Pampaloni, E.G. Reynaud, E.H.K. Stelzer, The third dimension bridges the gap between cell culture and live tissue, Nat. Rev. Mol. Cell Biol. 8 (2007) 839–845, https://doi.org/10.1038/nrm2236.

[59] M. Mandon, S. Huet, E. Dubreil, V. Fessard, L. Le Hégarat, Three-dimensional HepaRG spheroids as a liver model to study human genotoxicity in vitro with the single cell gel electrophoresis assay, Sci. Rep. 9 (2019) 10548, https://doi.org/10.1038/s41598-019-47114-7.

[60] M. Sendra, M. Štampar, K. Fras, B. Novoa, A. Figueras, B. Žegura, Adverse (geno) toxic effects of bisphenol A and its analogues in hepatic 3D cell model, Environ. Int. 171 (2023) 107721, https://doi.org/10.1016/j.envint.2022.107721.

[61] U.-K. Shah, J. de O. Mallia, N. Singh, K.E. Chapman, S.H. Doak, G.J.S. Jenkins, A three-dimensional in vitro HepG2 cells liver spheroid model for genotoxicity studies, Mutat. Res. Toxicol. Environ. Mutagen. 825 (2018) 51–58, https://doi.org/10.1016/j.mrgentox.2017.12.005.

[62] M. Štampar, S. Žabkar, M. Filipič, B. Žegura, HepG2 spheroids as a biosensor-like cell-based system for (geno)toxicity assessment, Chemosphere 291 (2022) 132805, https://doi.org/10.1016/j.chemosphere.2021.132805.

[63] S.V. Llewellyn, G.E. Conway, I. Zanoni, A.K. Jørgensen, U.-K. Shah, D.A. Seleci, J. G. Keller, J.W. Kim, W. Wohlleben, K.A. Jensen, A. Costa, G.J.S. Jenkins, M.J. D. Clift, S.H. Doak, Understanding the impact of more realistic low-dose, prolonged engineered nanomaterial exposure on genotoxicity using 3D models of the human liver, J. Nanobiotechnol. 19 (2021) 193, https://doi.org/10.1186/s12951-021-00938-w.

[64] K. Duval, H. Grover, L.-H. Han, Y. Mou, A.F. Pegoraro, J. Fredberg, Z. Chen, Modeling Physiological Events in 2D vs. 3D Cell Culture, Physiology 32 (2017) 266–277, https://doi.org/10.1152/physiol.00036.2016.

[65] C.S. Pridgeon, C. Schlott, M.W. Wong, M.B. Heringa, T. Heckel, J. Leedale, L. Launay, V. Gryshkova, S. Przyborski, R.N. Bearon, E.L. Wilkinson, T. Ansari, J. Greenman, D.F.G. Hendriks, S. Gibbs, J. Sidaway, R.L. Sison-Young, P. Walker, M.J. Cross, B.K. Park, C.E.P. Goldring, Innovative organotypic in vitro models for safety assessment: aligning with regulatory requirements and understanding models of the heart, skin, and liver as paradigms, Arch. Toxicol. 92 (2018) 557–569, https://doi.org/10.1007/s00204-018-2152-9.

[66] M. Štampar, J. Tomc, M. Filipič, B. Žegura, Development of in vitro 3D cell model from hepatocellular carcinoma (HepG2) cell line and its application for genotoxicity testing, Arch. Toxicol. 93 (2019) 3321–3333, https://doi.org/10.1007/s00204-019-02576-6.

[67] G.E. Conway, U.-K. Shah, S. Llewellyn, T. Cervena, S.J. Evans, A.S. Al Ali, G. J. Jenkins, M.J.D. Clift, S.H. Doak, Adaptation of the in vitro micronucleus assay for genotoxicity testing using 3D liver models supporting longer-term exposure durations, Mutagenesis 35 (2020) 319–330, https://doi.org/10.1093/mutage/geaa018.

[68] ATCC, Hep G2 [HEPG2] - HB-8065 | ATCC, (n.d.). ⟨https://www.atcc.org/products/hb-8065⟩ (accessed July 2, 2024).

[69] K.W.S.J. Fey, Determination of acute lethal and chronic lethal dose thresholds of valproic acid using 3D spheroids constructed from the immortal human hepatocyte cell line HepG2/C3A, 2013. ⟨http://www.scopus.com/inward/record.url?eid=2-s2.0-84891981522&partnerID=40&md5=51f161471a44133c487beaf1a17ac9a5⟩.

[70] H. Gaskell, P. Sharma, H.E. Colley, C. Murdoch, D.P. Williams, S.D. Webb, Characterization of a functional C3A liver spheroid model, Toxicol. Res. (Camb.). 5 (2016) 1053–1065, https://doi.org/10.1039/C6TX00101G.

[71] S.J. Fey, B. Korzeniowska, K. Wrzesinski, Response to and recovery from treatment in human liver-mimetic clinostat spheroids: a model for assessing repeated-dose drug toxicity, Toxicol. Res. (Camb.). 9 (2020) 379–389, https://doi.org/10.1093/toxres/tfaa033.

[72] ATCC, 2013, C3A [HepG2/C3A, derivative of Hep G2 (ATCC HB-8065)] (ATCC ® CRL-10741™), 2 (2013) 45200673⟨https://www.atcc.org/products/crl-3581#detailed-product-information⟩accessed July 2, 2024.

[73] J.E. Seo, X. He, L. Muskhelishvili, P. Malhi, N. Mei, M. Manjanatha, M. Bryant, T. Zhou, T. Robison, X. Guo, Evaluation of an In Vitro Three-Dimensional HepaRG Spheroid Model for Genotoxicity Testing Using the High-Throughput CometChip Platform, ALTEX 39 (2022) 583–604, https://doi.org/10.14573/altex.2201121.

[74] A.S. Serras, J.S. Rodrigues, M. Cipriano, A.V. Rodrigues, N.G. Oliveira, J. P. Miranda, A critical perspective on 3D liver models for drug metabolism and toxicology studies, Front. Cell Dev. Biol. 9 (2021), https://doi.org/10.3389/fcell.2021.626805.

[75] O. Sirenko, M.K. Hancock, J. Hesley, D. Hong, A. Cohen, J. Gentry, C.B. Carlson, D.A. Mann, Phenotypic characterization of toxic compound effects on liver spheroids derived from iPSC using confocal imaging and three-dimensional image analysis, Assay. Drug Dev. Technol. 14 (2016) 381–394, https://doi.org/10.1089/adt.2016.729.

[76] H.H.J. Gerets, K. Tilmant, B. Gerin, H. Chanteux, B.O. Depelchin, S. Dhalluin, F. A. Atienzar, Characterization of primary human hepatocytes, HepG2 cells, and HepaRG cells at the mRNA level and CYP activity in response to inducers and their predictivity for the detection of human hepatotoxins, Cell Biol. Toxicol. 28 (2012) 69–87, https://doi.org/10.1007/s10565-011-9208-4.

[77] Y. Park, K.M. Huh, S.W. Kang, Applications of biomaterials in 3d cell culture and contributions of 3d cell culture to drug development and basic biomedical research, Int. J. Mol. Sci. 22 (2021) 1–21, https://doi.org/10.3390/ijms22052491.

[78] S.C. Ramaiahgari, S. Waidyanatha, D. Dixon, M.J. DeVito, R.S. Paules, S. S. Ferguson, From the cover: three-dimensional (3D) HepaRG spheroid model with physiologically relevant xenobiotic metabolism competence and hepatocyte functionality for liver toxicity screening, Toxicol. Sci. 159 (2017) 124–136, https://doi.org/10.1093/toxsci/kfx122.

[79] Gibco, HepaRGTM Cells, Cryopreserved, (n.d.). ⟨https://www.thermofisher.com/order/catalog/product/HPRGC10⟩ (accessed July 2, 2024).

[80] R.M. Tostões, S.B. Leite, J.P. Miranda, M. Sousa, D.I.C. Wang, M.J.T. Carrondo, P. M. Alves, Perfusion of 3D encapsulated hepatocytes—A synergistic effect enhancing long-term functionality in bioreactors, Biotechnol. Bioeng. 108 (2011) 41–49, https://doi.org/10.1002/bit.22920.

[81] C.C. Bell, V.M. Lauschke, S.U. Vorrink, H. Palmgren, R. Duffin, T.B. Andersson, M. Ingelman-Sundberg, Transcriptional, functional, and mechanistic comparisons of stem cell–derived hepatocytes, HepaRG Cells, and three-dimensional human hepatocyte spheroids as predictive in vitro systems for drug-induced liver injury, Drug Metab. Dispos. 45 (2017) 419–429, https://doi.org/10.1124/dmd.116.074369.

[82] C.C. Bell, D.F.G. Hendriks, S.M.L. Moro, E. Ellis, J. Walsh, A. Renblom, L. Fredriksson Puigvert, A.C.A. Dankers, F. Jacobs, J. Snoeys, R.L. Sison-Young, R. E. Jenkins, Å. Nordling, S. Mkrtchian, B.K. Park, N.R. Kitteringham, C.E. P. Goldring, V.M. Lauschke, M. Ingelman-Sundberg, Characterization of primary human hepatocyte spheroids as a model system for drug-induced liver injury, liver function and disease, Sci. Rep. 6 (2016), https://doi.org/10.1038/srep25187.

[83] P.F. Pinheiro, S.A. Pereira, S.G. Harjivan, I.L. Martins, A.T. Marinho, M. Cipriano, C.C. Jacob, N.G. Oliveira, M.F. Castro, M.M. Marques, A.M.M. Antunes, J. P. Miranda, Hepatocyte spheroids as a competent in vitro system for drug biotransformation studies: nevirapine as a bioactivation case study, Arch. Toxicol. 91 (2017) 1199–1211, https://doi.org/10.1007/s00204-016-1792-x.

[84] K. Takayama, K. Kawabata, Y. Nagamoto, K. Kishimoto, K. Tashiro, F. Sakurai, M. Tachibana, K. Kanda, T. Hayakawa, M.K. Furue, H. Mizuguchi, 3D spheroid culture of hESC/hiPSC-derived hepatocyte-like cells for drug toxicity testing, Biomaterials 34 (2013) 1781–1789, https://doi.org/10.1016/j.biomaterials.2012.11.029.

[85] H. Rashidi, N.-T. Luu, S.M. Alwahsh, M. Ginai, S. Alhaque, H. Dong, R.A. Tomaz, B. Vernay, V. Vigneswara, J.M. Hallett, A. Chandrashekran, A. Dhawan, L. Vallier, M. Bradley, A. Callanan, S.J. Forbes, P.N. Newsome, D.C. Hay, 3D human liver tissue from pluripotent stem cells displays stable phenotype in vitro and supports compromised liver function in vivo, Arch. Toxicol. 92 (2018) 3117–3129, https://doi.org/10.1007/s00204-018-2280-2.

[86] F. Meier, N. Freyer, J. Brzeszczynska, F. Knï¿½spel, L. Armstrong, M. Lako, S. Greuel, G. Damm, E. Ludwig-Schwellinger, U. Deschl, J. Ross, M. Beilmann, K. Zeilinger, Hepatic differentiation of human iPSCs in different 3D models: a comparative study, Int. J. Mol. Med. (2017), https://doi.org/10.3892/ijmm.2017.3190.

[87] H. Qosa, A.J.S. Ribeiro, N.R. Hartman, D.A. Volpe, Characterization of a commercially available line of iPSC hepatocytes as models of hepatocyte function and toxicity for regulatory purposes, J. Pharmacol. Toxicol. Methods 110 (2021) 107083, https://doi.org/10.1016/j.vascn.2021.107083.

[88] G. Lee, H. Kim, J.Y. Park, G. Kim, J. Han, S. Chung, J.H. Yang, J.S. Jeon, D.-H. Woo, C. Han, S.K. Kim, H.-J. Park, J.-H. Kim, Generation of uniform liver spheroids from human pluripotent stem cells for imaging-based drug toxicity analysis, Biomaterials 269 (2021) 120529, https://doi.org/10.1016/j.biomaterials.2020.120529.

[89] Y. Fang, R.M. Eglen, Three-Dimensional Cell Cultures in Drug Discovery and Development, SLAS Discov. 22 (2017) 456–472, https://doi.org/10.1177/1087057117696795.

[90] W. Gao, D. Wu, Y. Wang, Z. Wang, C. Zou, Y. Dai, C.-F. Ng, J.Y.-C. Teoh, F. L. Chan, Development of a novel and economical agar-based non-adherent three-dimensional culture method for enrichment of cancer stem-like cells, Stem Cell Res. Ther. 9 (2018) 243, https://doi.org/10.1186/s13287-018-0987-x.

[91] T.-M. Achilli, J. Meyer, J.R. Morgan, Advances in the formation, use and understanding of multi-cellular spheroids, Expert Opin. Biol. Ther. 12 (2012) 1347–1360, https://doi.org/10.1517/14712598.2012.707181.

[92] E. Verjans, J. Doijen, W. Luyten, B. Landuyt, L. Schoofs, Three-dimensional cell culture models for anticancer drug screening: worth the effort? J. Cell. Physiol. 233 (2018) 2993–3003, https://doi.org/10.1002/jcp.26052.

[93] J. Varet, A. Barranger, C. Crochet, S. Huet, K. Hogeveen, L. Le Hégarat, V. Fessard, New methodological developments for testing the in vitro genotoxicity of nanomaterials: Comparison of 2D and 3D HepaRG liver cell

models and classical and high throughput comet assay formats, Chemosphere 350 (2023) 140975, https://doi.org/10.1016/j.chemosphere.2023.140975.

[94] S. Nath, G.R. Devi, Three-dimensional culture systems in cancer research: Focus on tumor spheroid model, Pharmacol. Ther. 163 (2016) 94–108, https://doi.org/10.1016/j.pharmthera.2016.03.013.

[95] K. Froehlich, J.-D. Haeger, J. Heger, J. Pastuschek, S.M. Photini, Y. Yan, A. Lupp, C. Pfarrer, R. Mrowka, E. Schleußner, U.R. Markert, A. Schmidt, Generation of multicellular breast cancer tumor spheroids: comparison of different protocols, J. Mammary Gland Biol. Neoplasia. 21 (2016) 89–98, https://doi.org/10.1007/s10911-016-9359-2.

[96] B. Pinto, A.C. Henriques, P.M.A. Silva, H. Bousbaa, Three-dimensional spheroids as in vitro preclinical models for cancer research, Pharmaceutics 12 (2020) 1186, https://doi.org/10.3390/pharmaceutics12121186.

[97] R.L.F. Amaral, M. Miranda, P.D. Marcato, K. Swiech, Comparative analysis of 3D bladder tumor spheroids obtained by forced floating and hanging drop methods for drug screening, Front. Physiol. 8 (2017), https://doi.org/10.3389/fphys.2017.00605.

[98] B.I. Biazi, T.A. Zanetti, L.A. Marques, A. Baranoski, G.C. Coatti, M.S. Mantovani, mRNAs biomarker related to the control of proliferation and cell death in HepG2/C3A spheroid and monolayer cultures treated with piperlongumine, Appl. Cancer Res. 40 (2020) 2, https://doi.org/10.1186/s41241-020-00086-x.

[99] K. Wrzesinski, S. Alnøe, H. H. Jochumsen, K. Mikkelsen, T. D. Bryld, J. S. Vistisen, P. Willems Alnøe, S. J. Fey, A Purpose-Built System for Culturing Cells as In Vivo Mimetic 3D Structures. in: Biomech. Funct. Tissue Eng., IntechOpen, 2021, https://doi.org/10.5772/intechopen.96091.

[100] A. Collins, P. Møller, G. Gajski, S. Vodenková, A. Abdulwahed, D. Anderson, E. E. Bankoglu, S. Bonassi, E. Boutet-Robinet, G. Brunborg, C. Chao, M.S. Cooke, C. Costa, S. Costa, A. Dhawan, J. de Lapuente, C.Del Bo', J. Dubus, M. Dusinska, S. J. Duthie, N.El Yamani, B. Engelward, I. Gaivão, L. Giovannelli, R. Godschalk, S. Guilherme, K.B. Gutzkow, K. Habas, A. Hernández, O. Herrero, M. Isidori, A. N. Jha, S. Knasmüller, I.M. Kooter, G. Koppen, M. Kruszewski, C. Ladeira, B. Laffon, M. Larramendy, L.Le Hégarat, A. Lewies, A. Lewinska, G.E. Liwszyc, A. L. de Cerain, M. Manjanatha, R. Marcos, M. Milić, V.M. de Andrade, M. Moretti, D. Muruzabal, M. Novak, R. Oliveira, A.-K. Olsen, N. Owiti, M. Pacheco, A. K. Pandey, S. Pfuhler, B. Pourrut, K. Reisinger, E. Rojas, E. Rundén-Pran, J. Sanz-Serrano, S. Shaposhnikov, V. Sipinen, K. Smeets, H. Stopper, J.P. Teixeira, V. Valdiglesias, M. Valverde, F. van Acker, F.-J. van Schooten, M. Vasquez, J. F. Wentzel, M. Wnuk, A. Wouters, B. Žegura, T. Zikmund, S.A.S. Langie, A. Azqueta, Measuring DNA modifications with the comet assay: a compendium of protocols, Nat. Protoc. 18 (2023) 929–989, https://doi.org/10.1038/s41596-022-00754-y.

[101] C. Chao, L.P. Ngo, B.P. Engelward, SpheroidChip: patterned agarose microwell compartments harboring HepG2 spheroids are compatible with genotoxicity testing, ACS Biomater. Sci. Eng. 6 (2020) 2427–2439, https://doi.org/10.1021/acsbiomaterials.9b01951.

[102] M. Fenech, Cytokinesis-block micronucleus cytome assay, Nat. Protoc. 2 (2007) 1084–1104, https://doi.org/10.1038/nprot.2007.77.

[103] M. Gerić, G. Gajski, V. Garaj-Vrhovac, γ-H2AX as a biomarker for DNA double-strand breaks in ecotoxicology, Ecotoxicol. Environ. Saf. 105 (2014) 13–21, https://doi.org/10.1016/j.ecoenv.2014.03.035.

[104] C.L. Li, T. Tian, K.J. Nan, N. Zhao, Y.H. Guo, J. Cui, J. Wang, W.G. Zhang, Survival advantages of multicellular spheroids vs. monolayers of HepG2 cells in vitro, Oncol. Rep. 20 (2008) 1465–1471, https://doi.org/10.3892/or_00000167.

[105] M. Štampar, T. Ravnjak, A.-M. Domijan, B. Žegura, Combined toxic effects of BPA and its two analogues BPAP and BPC in a 3D HepG2 cell model, Molecules 28 (2023) 3085, https://doi.org/10.3390/molecules28073085.

[106] C.F. Araujo-Lima, R. de C.C. Carvalho, R.B. Peres, L.F. de A. Fiuza, B.V.D. Galvão, F.S. Castelo-Branco, M.M. Bastos, N. Boechat, I. Felzenszwalb, M. de N.C. Soeiro, In silico and in vitro assessment of anti-Trypanosoma cruzi efficacy, genotoxicity and pharmacokinetics of pentasubstituted pyrrolic Atorvastatin-aminoquinoline hybrid compounds, Acta Trop. 242 (2023), https://doi.org/10.1016/j.actatropica.2023.106924.

[107] S. Mushtaq, K. Shahzad, T. Saeed, A. Ul-Hamid, B.H. Abbasi, N. Ahmad, W. Khalid, M. Atif, Z. Ali, R. Abbasi, Biocompatibility and cytotoxicity in vitro of surface-functionalized drug-loaded spinel ferrite nanoparticles, Beilstein J. Nanotechnol. 12 (2021) 1339–1364, https://doi.org/10.3762/bjnano.12.99.

[108] M.F. da Silva, L.V.A. de Lima, T.A. Zanetti, I. Felicidade, P.O. Favaron, S.R. Lepri, D.B. Lirio Rondina, M.S. Mantovani, Diosgenin increases BBC3 expression in HepG2/C3A cells and alters cell communication in a 3D spheroid model, Mutat. Res. Toxicol. Environ. Mutagen. 879–880 (2022) 503512, https://doi.org/10.1016/j.mrgentox.2022.503512.

[109] N.J. Coltman, B.A. Coke, K. Chatzi, E.L. Shepherd, P.F. Lalor, T. Schulz-Utermoehl, N.J. Hodges, Application of HepG2/C3A liver spheroids as a model system for genotoxicity studies, Toxicol. Lett. 345 (2021) 34–45, https://doi.org/10.1016/j.toxlet.2021.04.004.

[110] C. Calitz, J.H. Hamman, S.J. Fey, A.M. Viljoen, C. Gouws, K. Wrzesinski, A sub-chronic Xysmalobium undulatum hepatotoxicity investigation in HepG2/C3A spheroid cultures compared to an in vivo model, J. Ethnopharmacol. 239 (2019) 111897, https://doi.org/10.1016/j.jep.2019.111897.

[111] N.V. Senyavina, T.N. Gerasimenko, N.V. Pulkova, D.V. Maltseva, Transport and toxicity of silver nanoparticles in HepaRG cell spheroids, Bull. Exp. Biol. Med. 160 (2016) 831–834, https://doi.org/10.1007/s10517-016-3321-6.

[112] J.-E. Seo, Y. Le, J. Revollo, J. Miranda-Colon, H. Xu, P. McKinzie, N. Mei, T. Chen, R.H. Heflich, T. Zhou, T. Robison, J.A. Bonzo, X. Guo, Evaluating the mutagenicity of N-nitrosodimethylamine in 2D and 3D HepaRG cell cultures using error-corrected next generation sequencing, Arch. Toxicol. 98 (2024) 1919–1935, https://doi.org/10.1007/s00204-024-03731-4.

[113] J.-E. Seo, X. Li, Y. Le, N. Mei, T. Zhou, X. Guo, High-throughput micronucleus assay using three-dimensional HepaRG spheroids for in vitro genotoxicity testing, Arch. Toxicol. 97 (2023) 1163–1175, https://doi.org/10.1007/s00204-023-03461-z.

[114] J.-E. Seo, J.Z. Yu, H. Xu, X. Li, A.H. Atrakchi, T.J. McGovern, K.L.D. Bruno, N. Mei, R.H. Heflich, X. Guo, Genotoxicity assessment of eight nitrosamines using 2D and 3D HepaRG cell models, Arch. Toxicol. 97 (2023) 2785–2798, https://doi.org/10.1007/s00204-023-03560-x.

[115] C.C. Bell, A.C.A. Dankers, V.M. Lauschke, R. Sison-Young, R. Jenkins, C. Rowe, C. E. Goldring, K. Park, S.L. Regan, T. Walker, C. Schofield, A. Baze, A.J. Foster, D. P. Williams, A.W.M. van de Ven, F. Jacobs, J. van Houdt, T. Lähteenmäki, J. Snoeys, S. Juhila, L. Richert, M. Ingelman-Sundberg, Comparison of hepatic 2D sandwich cultures and 3d spheroids for long-term toxicity applications: a multicenter study, Toxicol. Sci. 162 (2018) 655–666, https://doi.org/10.1093/toxsci/kfx289.

[116] T. Hua, S. Kiran, Y. Li, Q.-X.A. Sang, Microplastics exposure affects neural development of human pluripotent stem cell-derived cortical spheroids, J. Hazard. Mater. 435 (2022) 128884, https://doi.org/10.1016/j.jhazmat.2022.128884.

[117] S.V. Llewellyn, G.E. Conway, U.-K. Shah, S.J. Evans, G.J.S. Jenkins, M.J.D. Clift, S.H. Doak, Advanced 3D liver models for in vitro genotoxicity testing following long-term nanomaterial exposure, J. Vis. Exp. (2020), https://doi.org/10.3791/61141.